

Milky Way demographics with the VVV survey[★]

II. Color transformations and near-infrared photometry for 136 million stars in the southern Galactic disk

M. Soto¹, R. Barbá^{1,2}, G. Gunthardt^{1,3}, D. Minniti^{4,5,6,7,8,9}, P. Lucas¹⁰, D. Majaess¹¹, M. Irwin¹², J. P. Emerson¹³, E. Gonzalez-Solares¹², M. Hempel^{4,8}, R. K. Saito^{4,8,14}, S. Guorovich^{3,15}, A. Roman-Lopes¹, C. Moni-Bidin^{16,17}, M. V. Santucho³, J. Borissova^{8,14}, R. Kurtev¹⁴, I. Toledo^{4,18}, D. Geisler¹⁶, M. Dominguez^{3,15}, and J. C. Beamin⁴

¹ Departamento de Física, Universidad de La Serena, 980 Benavente, La Serena, Chile
e-mail: msoto@dful.s.cl

² Instituto de Ciencias Astronómicas, del la Tierra y del Espacio (ICATE-CONICET), Av. España Sur 1512, J5402DSP San Juan, Argentina

³ Observatorio Astronómico de Córdoba, Universidad Nacional de Córdoba, Laprida 854, x5000 BGR, Córdoba, Argentina

⁴ Departamento de Astronomía y Astrofísica, Pontificia Universidad Católica de Chile, Vicuña Mackenna 4860, Casilla 306, Santiago 22, Chile

⁵ Vatican Observatory, Vatican City State 00120, Italy

⁶ European Southern Observatory, 3107 Vitacura, Santiago, Chile

⁷ Department of Astrophysical Sciences, Princeton University, Princeton NJ 08544-1001, USA

⁸ The Milky Way Millennium Nucleus, Av. Vicuña Mackenna 4860, 782-0436 Macul, Santiago, Chile

⁹ Departamento de Ciencia Físicas, Universidad Andrés Bello, Avda. República 252, Santiago, Chile

¹⁰ Centre for Astrophysics Research, Science and Technology Research Institute, University of Hertfordshire, Hatfield AL10 9AB, UK

¹¹ Department of Astronomy and Physics, Saint Mary's University, Halifax, Nova Scotia, B3K 5L3, Canada

¹² Institute of Astronomy, University of Cambridge, Madingley Road, Cambridge CB3 0HA, UK

¹³ Astronomy Unit, School of Physics and Astronomy, Queen Mary University of London, Mile End Road, London, E1 4NS, UK

¹⁴ Departamento de Física y Astronomía, Universidad de Valparaíso, Av. Gran Bretaña 1111, Playa Ancha, Casilla 5030, Chile

¹⁵ Instituto de Astronomía Teórica y Experimental, CONICET, Laprida 922, 5000 Córdoba, Argentina

¹⁶ Departamento de Astronomía, Universidad de Concepción, Casilla 160-C, Concepción, Chile

¹⁷ Instituto de Astronomía, Universidad Católica del Norte, Av. Angamos 0610, Antofagasta, Chile

¹⁸ Atacama Large Millimeter Array, Alonso de Córdova 3107, Vitacura, Santiago, Chile

Received 18 July 2012 / Accepted 25 January 2013

ABSTRACT

The new multi-epoch near-infrared VISTA Variables in the Vía Láctea (VVV) survey is sampling 562 deg² of the Galactic bulge and adjacent regions of the disk. Accurate astrometry established for the region surveyed allows the VVV data to be merged with overlapping surveys (e.g., GLIMPSE, WISE, 2MASS, etc.), thereby enabling the construction of longer baseline spectral energy distributions for astronomical targets. However, in order to maximize use of the VVV data, a set of transformation equations are required to place the VVV *JHK* photometry onto the 2MASS system. The impetus for this work is to develop those transformations via a comparison of 2MASS targets in 152 VVV fields sampling the Galactic disk. The transformation coefficients derived exhibit a reliance on variables such as extinction. The transformed data were subsequently employed to establish a mean reddening law of $E_{J-H}/E_{H-K_s} = 2.13 \pm 0.04$, which is the most precise determination to date and merely emphasizes the pertinence of the VVV data for determining such important parameters.

Key words. Galaxy: disk – Galaxy: stellar content – Galaxy: structure – infrared: stars – surveys

1. Introduction

The fields of the southern Galactic disk are complicated regions to research. Near the Galactic plane the interstellar medium (ISM) is rich, complex, and dust extinction is extreme and inhomogeneous at small scales. Moreover, the surface density of sources reaches a maximum in the Galactic plane. Fields exhibiting one star brighter than $K_s = 18$ are catalogued every few square arcsec. Owing to the aforementioned factors, existing

optical and low-spatial resolution surveys have thus been inefficient at characterizing populations in the southern Galactic disk. Hence the importance of the VISTA Variables in the Vía Láctea (VVV) survey (Minniti et al. 2010; Saito et al. 2012), which is a near-infrared ESO public survey that is sampling 562 deg² of the Galactic bulge and adjacent regions of the disk. The survey is being carried out via the VISTA telescope, and images are being acquired through 5 broadband filters. The VVV fields examined here overlap with the GLIMPSE survey, which acquired images at 3.6, 4.5, 5.8 and 8 μm. Thus the sources surveyed will have multiband photometry ranging from the near to mid-infrared.

[★] Based on observations taken within the ESO VISTA Public Survey VVV, Programme ID 179.B-2002.

Latitude	+2	1	0	-1	-2
152	151	150	149	148	147
151	150	149	148	147	145
150	149	148	147	145	144
149	148	147	146	145	143
148	147	146	145	143	142
147	146	145	144	142	141
146	145	144	143	141	140
145	144	143	142	140	139
144	143	142	141	139	138
143	142	141	140	138	137
142	141	140	139	136	135
141	140	139	138	134	133
140	139	138	137	132	131
139	138	137	136	131	130
138	137	136	135	129	128
137	136	135	134	128	127
136	135	134	133	127	126
135	134	133	132	126	125
134	133	132	131	125	124
133	132	131	130	124	123
132	131	130	129	123	122
131	130	129	128	122	121
130	129	128	127	121	120
129	128	127	126	120	119
128	127	126	125	119	118
127	126	125	124	117	116
126	125	124	123	116	115
125	124	123	122	115	
124	123	122	121		
123	122	121			
122	121				
121					
120					
119					
118					
117					
116					
115					

Fig. 1. Galactic disk fields imaged by the VVV survey. The VVV disk tile names start with d, followed by the numbering as shown in the figure.

The region sampled is of particular interest for ISM studies because the 4th Galactic quadrant hosts the Coal Sack, in tandem with several prominent nebulae and areas exhibiting large star formation rates (SFR). The inner disk region includes large numbers of open clusters (Borissova et al. 2011; Bica et al. 2008; Kharchenko et al. 2005 and references therein) and associations, which allows for detailed stellar population studies. The near-infrared nature of the surveys is particularly pertinent for such analyses since such photometry is less sensitive to dust obscuration than optical observations, thus permitting greater penetration into the disk. The line of sight depth in the 1st and 4th Galactic quadrants is large, and nearby foreground dwarf stars are mixed with distant red giants along a given line of sight. In addition, the region sampled is pertinent for Galactic structure studies, as there is presently no consensus on the number or delineation of the Galaxy’s major spiral arms (Benjamin et al. 2008; Majaess et al. 2009), and the tail end of the long bar is undercharacterized (Fig. 7 in Majaess 2010).

Prior to VVV the 2MASS survey (Skrutskie et al. 2006) has been the main near-infrared photometric survey covering much of the Galactic plane, and many models and data in the 2MASS photometric system have appeared in the literature. In comparing with this previous work it is therefore useful, at least until sufficient modeling is available in the VISTA photometric system, to know the 2MASS equivalent magnitudes to the actual VISTA magnitudes. In addition, such transformations allow to combine the information of both surveys to reach a wider magnitude range (e.g. saturated stars in the VVV catalogues can be complemented with the 2MASS magnitudes once they are transformed to the 2MASS system). However we note that, for the greatest accuracy, transformations between different photometric systems should in general be avoided as they will always be dependent on the (usually unknown) spectrum of the objects, but pending availability of more models in the VISTA system we find that it is expedient to estimate what VISTA magnitudes would be in the 2MASS system.

Carpenter et al. (2001) produced transformation equations to convert colors and magnitudes from AAO, ARNICA, CIT, DENIS, ESO, LCO, MSSO, SAAO and UKIRT photometric systems to 2MASS. This paper follows a similar procedure to obtain transformations linking the VVV and 2MASS systems. A well defined set of transformation equations should be valid over a large color baseline (i.e. $-0.5 \leq (J - K_s) \leq 4.0$) owing to the high (and strongly varying) reddening values, and the presence of (bluer) dwarfs and (redder) giants. In this work we present empirical JHK_s color transformations for 152 tiles completed during year 1 (2010), photometric catalogue version 1.1 (see observation schedule in Minniti et al. 2010), between the VISTA and 2MASS photometric systems. The calibrations were inferred from VVV sources in the southern Galactic disk in the region bounded by $-65.3^\circ \leq l \leq -10.0^\circ$ and $-2.25^\circ \leq b \leq +2.25^\circ$, and apply to all the VVV photometry derived from the Cambridge Astronomical Survey Unit (CASU) catalogues in this area.

This paper is organized as follows: in Sect. 2 a brief overview is provided of the VVV observations and the CASU pipeline, which produces the photometric catalogues. Section 3 explains

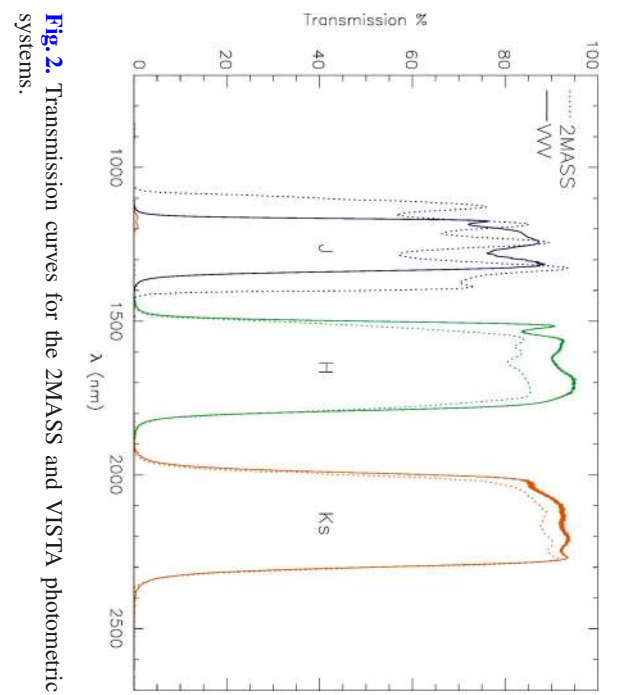


Fig. 2. Transmission curves for the 2MASS and VISTA photometric systems.

the selection procedure for the subsample of VVV-2MASS stars used to derive the photometric transformations. Finally, Sect. 4 contains the discussion of the transformation coefficients obtained, while our conclusions are summarized in Sect. 5.

2. Observations

2.1. VVV Observations

Near-infrared VVV observations were acquired via VISTA (Visible and Infrared Survey Telescope for Astronomy), which is stationed at the Paranal Observatory. VISTA is a 4 m telescope equipped with the VIRCAM instrument (VISTA InfraRed Camera; Emerson et al. 2006). Each VVV field (called a *tile*) covers 1.64 deg^2 . There are 152 tiles covering about 250 deg^2 of the Galactic disk (Fig. 1). The VVV tiles exhibit overlap between consecutive blocks, and for the complete survey the overlap sums to $\sim 42 \text{ deg}^2$. The equatorial and Galactic coordinates for the center of each tile are listed in Table A.1 of Saito et al. (2012). The VISTA IR mosaic camera has a 1.65 deg diameter field of view, that is sampled with $16 \text{ Raytheon } 2048 \times 2048$ arrays (Dalton et al. 2006). The detectors have $0.339''$ pixels which produce a 0.6 deg^2 field per pointing. Each pointing is called a “pawprint”, with spacings of 42% and 90% between the detectors along the X and Y axes, respectively, where 6 overlapping pawprints are used to build a tile.

The VVV survey includes observations of the complete survey area in the 5 available filters, i.e. Z, Y, J, H, and K_s . As described by Minniti et al. (2010), these multi-band observations were scheduled to be carried out during the first year of the survey (2010), but were partly carried over into 2011 owing to various factors. The principal part of the survey (year 2–5) will be a K_s -band variability study.

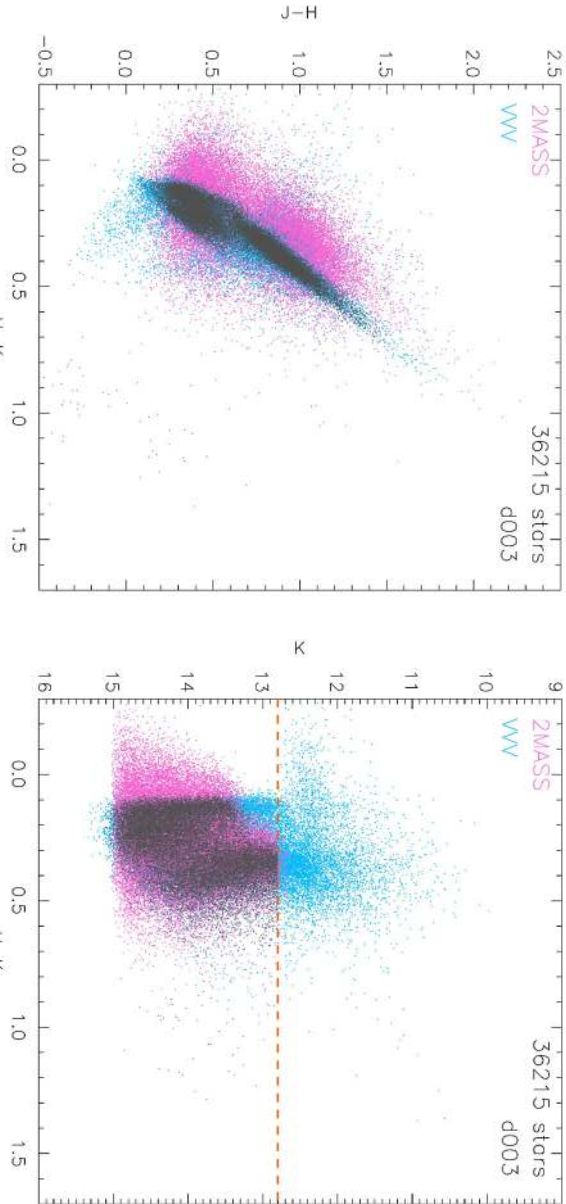


Fig. 3. Color–color and color–magnitude diagrams for the tile *d003*. VVV data (blue dots) have been matched with 2MASS data on the same field (pink dots), where a subsample has been chosen to calculate the coefficients (dark grey). A limiting magnitude (orange dashed line) in each band has been used to avoid saturated VVV stars.

2.2. CASU pipeline: photometry

The reduction of IR data is far more complex than reducing optical data. IR detectors are more unstable than optical detectors and sky emission can be several magnitudes brighter than many IR stellar sources (Lewis et al. 2010), and marginally fainter than the saturation limit. In the case of VVV, the limiting magnitude for the aperture photometry of the catalogues appears at $K_s = 18$ mag in most fields in the disk, with an expected sky brightness at the VISTA site of $K_s \approx 13.0$ mag (Cuby et al. 2000). Moreover, IR sky emission varies over short timescales, and changes in spatial scale can be large or small depending on the instrument. Consequently, short exposures are needed, which subsequently increases the amount of information acquired each night. Thus, surveys like VVV require automated pipelines to process the large volumes of nightly data. The VISTA Data Flow System pipeline running at CASU handles the data processing¹.

Zeropoints on the VISTA system are determined using the 2MASS data following a procedure similar to that described for WFCAM (Hodgkin et al. 2005). A color selected set of 2MASS stars lying in each pawprint are chosen and their magnitudes on the VISTA photometric system are calculated using the following color equations for data release 1.1 (we adopt $K = K_s$ in the equations for simplicity):

$$\begin{aligned} J_{\text{VVV}} &= J_{\text{2MASS}} - 0.077(J_{\text{2MASS}} - H_{\text{2MASS}}), \\ H_{\text{VVV}} &= H_{\text{2MASS}} + 0.032(J_{\text{2MASS}} - H_{\text{2MASS}}), \\ K_{\text{VVV}} &= K_{\text{2MASS}} + 0.010(J_{\text{2MASS}} - K_{\text{2MASS}}). \end{aligned}$$

An extinction correction, based on Schlegel et al. (1998; henceforth SFD), is applied according to the prescription of Bonifacio et al. (2000). The corrections can be found in the CASU website². The analysis presented here is based on the derived colors and magnitudes established by the CASU pipeline. A detailed

account of the CASU pipeline can be found in Irwin et al. (2004), and will not be repeated here.

3. Procedures

3.1. Catalogue construction and 2MASS matching

The VISTA and 2MASS photometric systems do not exactly match, as expected given the observations were carried out at different sites with different telescopes, IR cameras, detectors and filters. Figure 2 shows a comparison of the transmission curves for both photometric systems. As discussed earlier we wish to determine, on a tile by tile basis, the transformations between the VISTA and 2MASS systems for VVV data in the Galactic disk. That is equivalent to changing the CASU calibration for each tile. Nevertheless, the revised transformations should be more robust since red objects will be included in the calibration, whereas the CASU calibration relies principally on blue stars.

The first step in obtaining the transformations was to select a set of VVV and 2MASS observations exhibiting solid photometry. A series of constraints were placed on the 2MASS and VVV photometry to account for undesirable effects arising from crowding and saturation. Extended sources were excluded. The procedure used to obtain a 2MASS–VVV catalogue for each tile can be summarized as follows:

- (a) Only sources with VVV K_s photometry defined as “stellar” (sources with a Gaussian sigma parameter between 0.9 and 2.2) were analyzed. This parameter is derived from the three intensity weighted second moments. K_s photometry was chosen since the data extend deeper than J or H for sources in the Galactic plane. Accounting for crowding effects in K_s provides a corresponding solution for the shallower J and H data.
- (b) Using the new list of K_s photometry, sources in close proximity to each other are subsequently culled, that is, stars exhibiting $r < 2''.0$ (i.e. the 2MASS pixel size) and whose magnitudes display less than a 2 magnitude differential with respect to the brightest star.

¹ For more details, see

<http://casu.ast.cam.ac.uk/surveys-projects/vista/technical/photometric-properties>

² <http://casu.ast.cam.ac.uk/surveys-projects/vista/technical/photometric-properties>

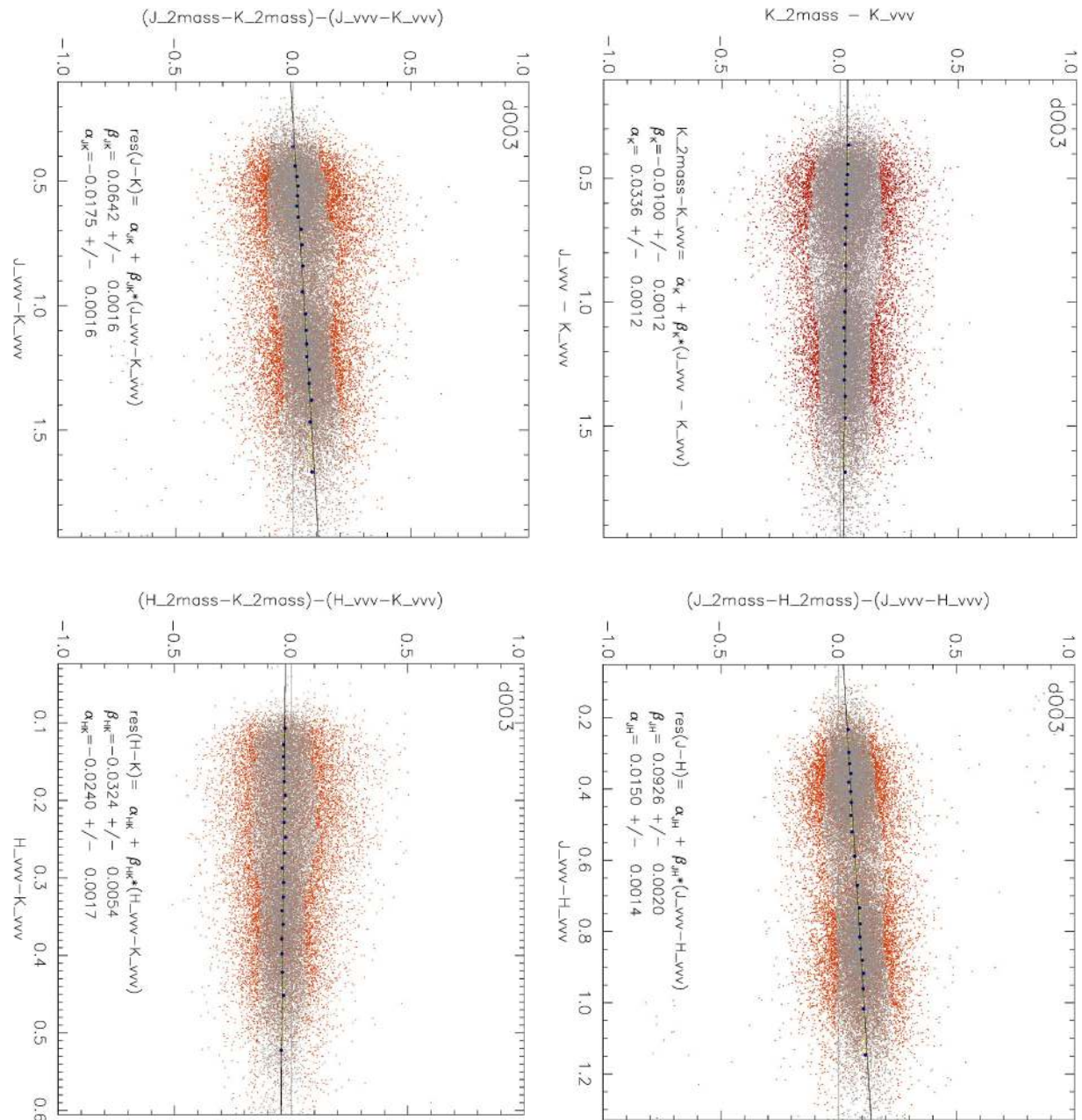


Fig. 4. Comparison of 2MASS and VVV photometry for stars observed in tile/field *d003*. In each case an iterative clipping algorithm has been applied to each one of the 20 adaptive bins of the distribution. The selected stars of the clipping algorithm (grey) have been used to calculate the linear fit, and the individual photometric uncertainties of each star were considered.

(c) The resulting catalogue is then matched with 2MASS, where only stars with photometric quality flag “A” or “B” in a radius of $0''.3$ are selected. For JHK_s data the 2MASS photometric quality flags “A” and “B” correspond to $S/NR > 10$ and $S/NR > 7$, respectively.

(d) The final list is constructed by cross-referencing the VVV K_s and 2MASS JHK_s list, received from the previous step, with the rest of the VVV J and H data matched using a radius of $0''.1$.

Once a clean VVV-2MASS catalogue has been created for each VVV tile, the transformation equations were derived. The procedure is similar to that employed by Carpenter (2001). Linear fits for the variables were determined, namely: $(K_s)_{\text{2MASS}} - (K_s)_{\text{VVV}}$ versus $(J - K_s)_{\text{VVV}}$, $(J - H)_{\text{2MASS}}$ versus $(J - H)_{\text{VVV}}$, $(J - K_s)_{\text{2MASS}}$ versus $(J - K_s)_{\text{VVV}}$, and $(H - K_s)_{\text{2MASS}}$ versus $(H - K_s)_{\text{VVV}}$ and coefficients (α_K, β_K) , $(\alpha_{JH}, \beta_{JH})$, $(\alpha_{JK}, \beta_{JK})$ and $(\alpha_{HK}, \beta_{HK})$,

respectively. Thus, the derived linear fits correspond to the equations:

$$K_{\text{2MASS}} - K_{\text{VVV}} = (J_{\text{vvv}} - K_{\text{vvv}}) \beta_K + \alpha_K, \quad (1)$$

$$(J_{\text{2MASS}} - H_{\text{2MASS}}) - (J_{\text{vvv}} - H_{\text{vvv}}) = (J_{\text{vvv}} - H_{\text{vvv}}) \beta_{JH} + \alpha_{JH}, \quad (2)$$

$$(J_{\text{2MASS}} - K_{\text{2MASS}}) - (J_{\text{vvv}} - K_{\text{vvv}}) = (J_{\text{vvv}} - K_{\text{vvv}}) \beta_{JK} + \alpha_{JK}, \quad (3)$$

$$(H_{\text{2MASS}} - K_{\text{2MASS}}) - (H_{\text{vvv}} - K_{\text{vvv}}) = (H_{\text{vvv}} - K_{\text{vvv}}) \beta_{HK} + \alpha_{HK}. \quad (4)$$

An iterative clipping algorithm was applied to reject stars beyond 2.5σ for each adaptive bin (i.e. uniformly populated bins). That allowed us to establish a robust determination of the coefficients for the photometric transformation in each case. A limiting magnitude was applied to each filter during the calculation

Table 1. Correlation coefficients between 2MASS-VVV transformation coefficients and $E(B - V)$.

Coeff	r_S^a	$\text{Prob}(r_S)^b$
α_K	0.289	3.026e-04
β_K	-0.395	4.425e-07
α_{JH}	0.424	5.209e-08
β_{JH}	-0.549	2.562e-13
α_{JK}	-0.183	2.397e-02
β_{JK}	-0.115	1.584e-01
α_{HK}	-0.692	5.682e-23
β_{HK}	0.708	1.886e-24

Notes. ^(a) Spearman’s correlation coefficient. ^(b) Significance of the correlation.

of the transformations, which ensures that saturated photometry was avoided. The limiting magnitudes used during the procedure were 13.8, 12.8 and 12.8, for J , H and K_s respectively. An example of the color–color and color–magnitude diagrams (CMD) in both photometric systems for tile $d003$ is shown in Fig. 3, whereas the result of the fitting procedure is shown in Fig. 4.

4. Discussion

Figure 5 displays the color–color diagram of tile $d003$, where the calculated transformations were applied to the respective VVV colors. The Gaussian fitting applied to the histograms of the JHK_s magnitude residuals, in our transformations for tile $d003$ exhibits $\sigma \approx 0.05$ mag for stars in the upper 25% of the magnitude range used to calculate the photometric transformations. These residuals are dominated by the 2MASS magnitude dispersion, where 2MASS photometric errors are typically several times higher (~ 6 on average for this tile) than those in the VVV catalogues.

Table A.1 lists the coefficients obtained for the 152 VVV tiles, while Fig. 6 displays the same coefficients as a function of Galactic longitude and latitude. Similarly, Tables B.1 and B.2 show the derived coefficients per tile for subsamples dominated by main sequence and post main sequence stars respectively. At first glance, the figures suggest a non-random behavior that is presumably related to the structure of the Milky Way. In order to test that hypothesis, we compared how the coefficients varied for low (red, $|b| \lesssim 1^\circ$) and high Galactic latitude fields (green, $2.1^\circ \gtrsim |b| \gtrsim 1^\circ$). For each subsample we fitted a fourth-order polynomial. A clear distinction between high- and low-latitude fields is observed in the photometric coefficients, with the apparent exception of the β_{JK} parameter. A similar analysis can be drawn by dividing the sample in low longitude (red, $l \geq 320^\circ$) and high longitude fields (green, $l < 320^\circ$). Where we have fitted a third-order polynomial to fit the subsamples in each case.

The variations of the transformation coefficients across the Galaxy may be caused by multiple effects, as discussed below.

4.1. Extinction on the disk for the VISTA fields

Extinction in the Galactic plane can be extreme and uneven at small scales. As mentioned, an extinction correction was employed in the VISTA pipeline based in part on the SFD map. The problems of SFD in regions of high extinction are well documented. Arce & Goodman (1999) evaluated the reliability of the SFD maps in the Taurus Dark Cloud complex, using 4 separate methods. Their results demonstrate a consistent overestimation by a factor of 1.3 to 1.5 in regions of smooth extinction

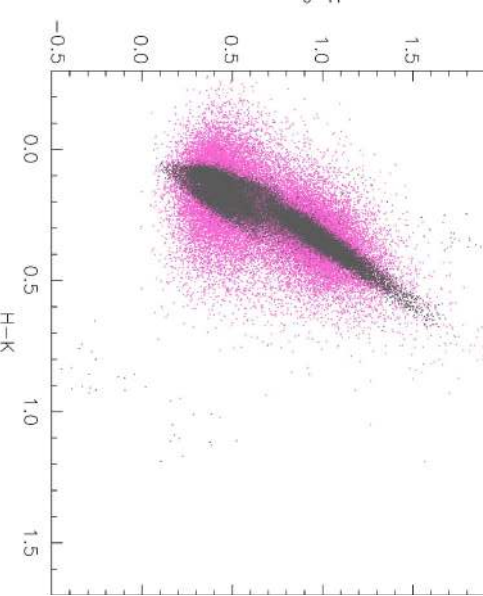


Fig. 5. Color–color diagram for VVV stars transformed to the 2MASS photometric system for tile $d003$. The transformation equations derived in Fig. 4 have been applied to the VVV colors (grey). The same stars featured in the 2MASS catalogue are overplotted (pink).

and $A_V > 0.5$ mag. By contrast, reddening values were underestimated in regions with steep extinction gradients. Subsequent studies have shown similar results in globular clusters (see Majewski et al. 2011 and references therein), whereby reddening values were overestimated by factors of 1.2 to 1.5. Moreover, the comparison between Majewski et al. (2011) extinction map, based on 2MASS (NIR)/Spitzer-IRAC observations, and the SFD map revealed clear discrepancies. Majewski et al. (2011) attributed the offset to the fact that long wavelength ($100\,\mu\text{m}$) infrared dust emission is not a viable tracer of dust extinction (SFD maps). A similar result was found recently using VVV data. Gonzalez et al. (2012) compared their bulge extinction map with the SFD map, and a significant difference appeared for $|b| < 6^\circ$. In addition to the limitations of the applied SFD maps, offsets in the photometric transformations are expected owing to the different filters employed by 2MASS and VVV. Thus the transformations may be affected by reddening and spectral type. Figure 7 illustrates that effect via a comparison of Padova isochrones (Girardi et al. 2000, 2002) on the 2MASS and VISTA photometric systems. In that example an old disk population (~ 10 Gyr; Carraro et al. 1999) affected by high extinction ($A_V \sim 10$) displays divergent colors.

Figure 8 and Table 1 show the photometric coefficients for 152 tiles as a function of the reddening used in the zeropoint correction for each tile, and their respective correlation results (r_S is the Spearman’s rank order correlation coefficient). The calculated correlations are significant in most of the coefficients, only β_{JK} and α_{JK} show little dependence on $E(B - V)$. Thus these results confirm our original assessment regarding the influence of extinction (see also Fig. 6). Since 2MASS and VVV colors and magnitudes must coincide for $A0V$ spectral type and $E(B - V) = 0$, as Fig. 7 shows, our photometric transformations should follow consistent relations when extrapolated to zero reddening. As expected, the linear fits for the α coefficients tend to zero for $E(B - V) = 0$, an effect that seems to grow stronger with the correlation r_S . Similarly, and in spite of the dispersion observed, these plots show a rough agreement with the inverse

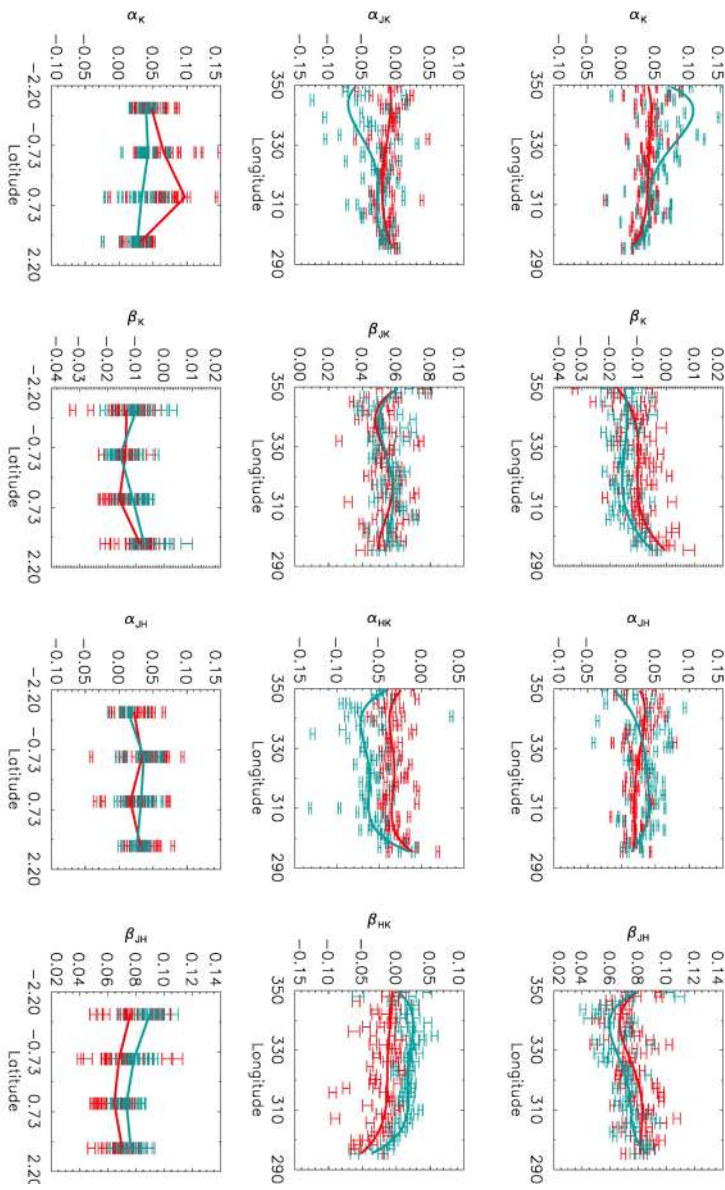


Fig. 6. Coefficients of the VVV-2MASS transformations as a function of Galactic longitude and latitude for 152 VVV tiles in the Galactic disk. Top and second row, we divided the sample into low (red; $|b| \lesssim 1^\circ$) and high latitude fields (green; $2.1^\circ \gtrsim |b| \gtrsim 1^\circ$). A fourth order polynomial was fitted in each case. Third and bottom row, photometric coefficients divided into low longitude (red; $l \gtrsim 320^\circ$), and high longitude fields (green; $l \lesssim 320^\circ$).

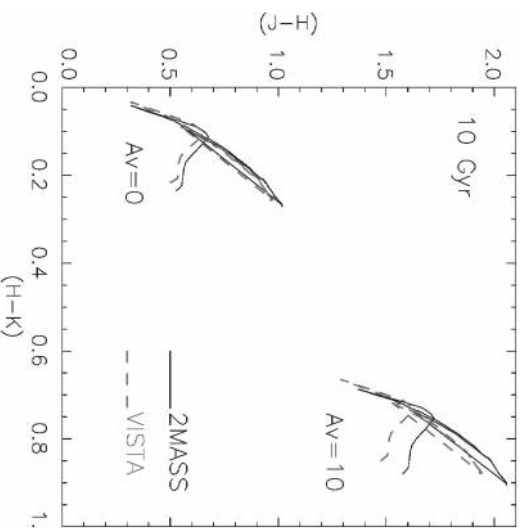


Fig. 7. Comparison of isochrones in the 2MASS (black) and VISTA (grey) photometric systems for a 10 Gyr population ($Z = 0.019$) observed through two extinction values ($Av = 0$ and $Av = 10$).

transformations that can be derived from the CASU equations (without their extinction corrections) in Sect. 2.2; which produce

$\beta_{JK} = 0.075$ and $\beta_{JH} = 0.109$ for $E(B-V) = 0$, as can be seen in Fig. 8. All this confirms the reliability of the photometric transformations obtained.

4.2. Mapping the Galactic disk with VVV

Figure 9 hosts the color-magnitude and color-color diagram for all fields in the VVV catalogue with VVV-2MASS color transformations. The diagram features 88 million stars obtained from our combined JHK_s catalogues of the Galactic disk. The combined CMD reveals the saturated population around $K_s \sim 10$ mag. However, our tests with individual tile-catalogues implied that saturation was typically near $K_s \sim 13$ mag (Fig. 4).

The combined color-color diagram can be used to calculate the infrared color-excess ratio (Indebetouw et al. 2005). The measured color excess ratio in our diagram is $E(J-H)/(E(H-K)) = 2.13 \pm 0.04$, which was inferred from the VVV data converted to the 2MASS system with $1.5 \geq (H-K_s) \geq 0.5$. The corresponding value in the original VISTA system is $E(J-H)/(E(H-K)) = 2.02 \pm 0.04$. These reddening laws are in general agreement with previously reported values for numerous lines of sight toward the inner Galaxy (Straizys & Laugalyt 2008; Majaess et al. 2011).

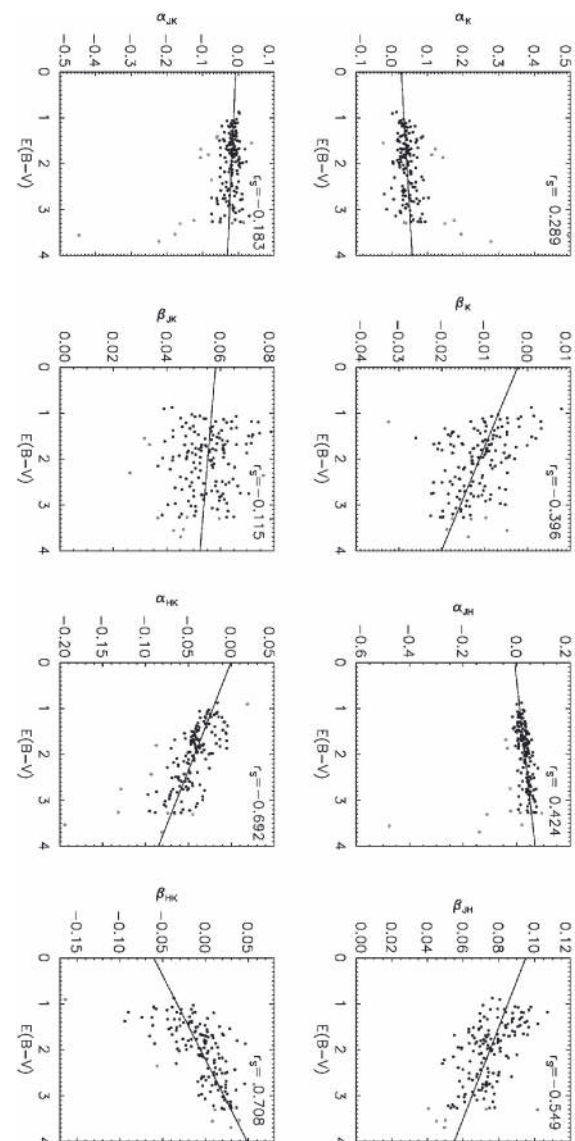


Fig. 8. Coefficients of the VVV-2MASS transformations as a function of the reddening used to correct the zeropoint for 152 VVV fields in the Galactic disk. We included in each plot a linear fit with an iterative clipping algorithm similar to that used to calculate the photometric transformations. Grey points are those rejected during the clipping procedure. Moreover, the Spearman's rank order correlation coefficient r_s has been calculated in each case.

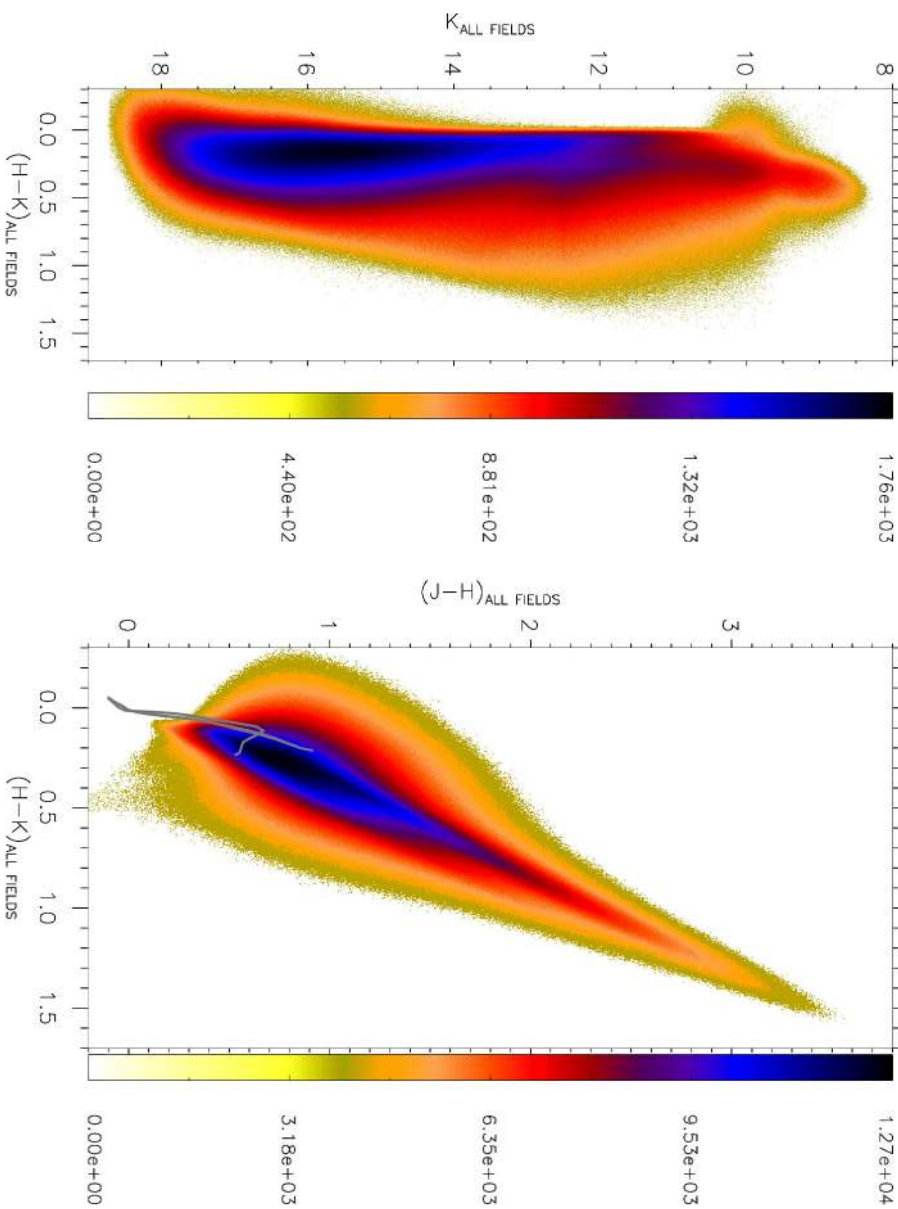


Fig. 9. Binned color-magnitude and color-color diagrams for all sources defined as stellar in the VVV catalogues (86 millions), which constitutes 152 tiles of the Galactic disk. Magnitudes have been transformed to the 2MASS photometric system in each tile using the respective coefficients. The CMD has been calculated at a resolution of 500×1600 bins, which corresponds to a binsize of 0.005 mags/bin. Similarly, our color-color diagram for the tiles of the Galactic disk was constructed at a resolution of 400×800 bins and the same binsize of the binned CMD. The latter includes an unreddened 0.05 Gyr isochrone (grey solid line) in the 2MASS system for reference.

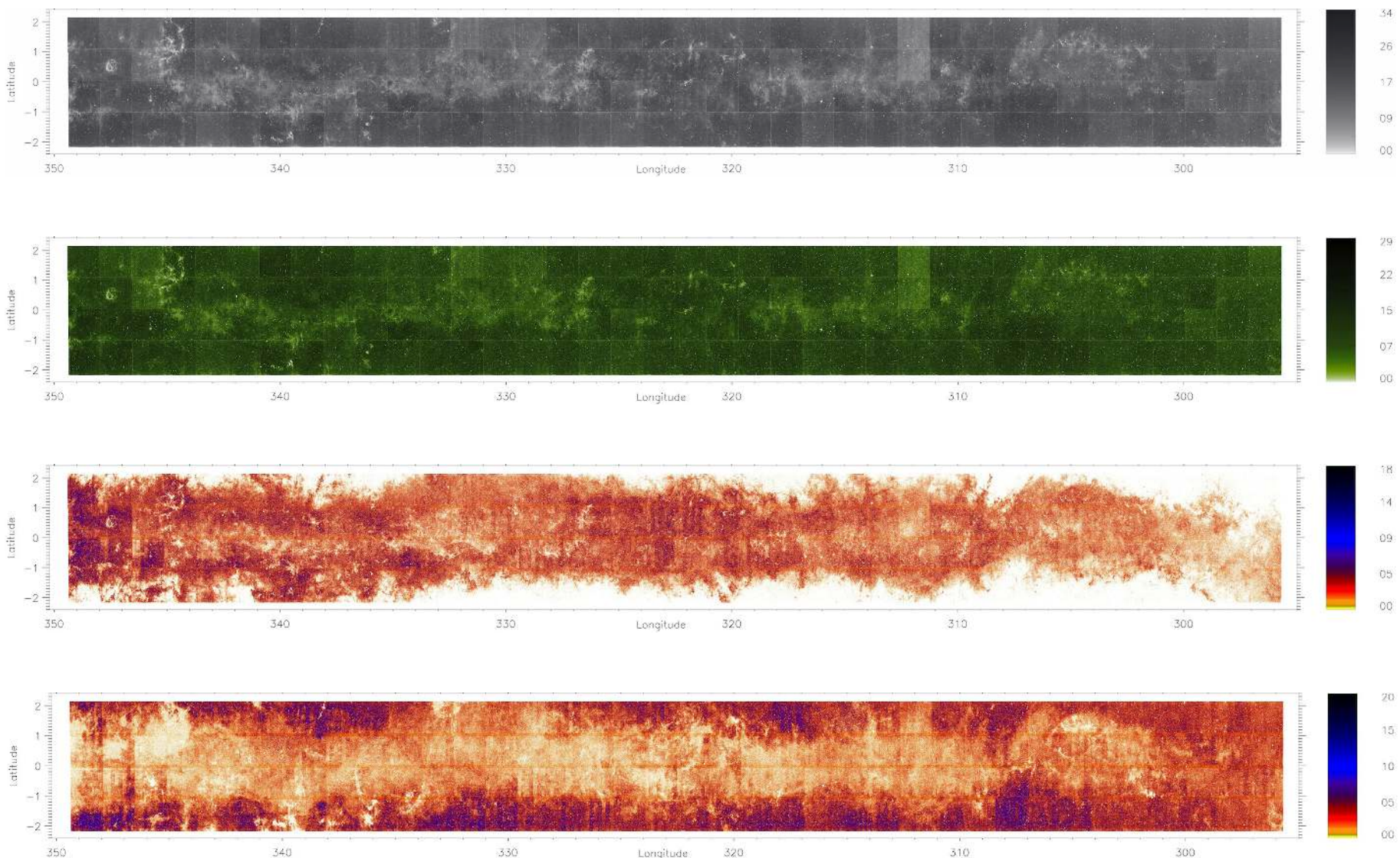


Fig. 10. Map featuring the number of sources or the disk tiles (152 fields) in VVV with a $0.005^\circ \times 0.005^\circ$ bin/pixel size. *Top*, map for all the sources in our combined JHK_s catalogues, 136 million sources. *Second row*, map for all the stellar sources, 88 million stars. *Third row*, map for stellar sources for the objects lying in a stripe in the color–color diagram defined by $(H - K) \times 1.97 + 0.54 \geq (J - H) \geq (H - K) \times 1.97 + 0.24$ and $(H - K) \geq 0.4$; this selection should be dominated by disk red giants with high extinction. *Bottom*, same as before, but for $(H - K) \leq 0.4$; the population selected in this starcount map should be dominated by red-giants and some main sequence stars with low extinction.

Figure 10 shows the source-count maps for all tiles processed for this work. Duplications in the overlapping regions between tiles have been avoided in the starcount maps, as in the CMD and color–color diagrams, by constructing simultaneously the three corresponding binned plots (CMD, color–color diagram and starcount map). Once a pixel has been used in the starcount map, only counts from the same tile will be accepted in the three binned plots. The first of these count maps in Fig. 10 includes

all 136×10^6 detected sources in the 152 tiles, regardless of their classification. The second map consists only of stellar sources (88×10^6 objects). There exist differences in the general number of counts per tile which we attribute to variations in the observation conditions between the tiles, in addition to patchy disk obscuration. Similarly, a marginal vertical stripe pattern is observed in many tiles. That pattern is a known background variation related to the construction of the tiles from the 6 pawprint images. As expected, when compared with the map including just stellar sources (second row), the general map including all the sources (top) displays more detailed structure in regions where diffuse sources are expected. Finally, for the last two starcount maps, we selected two subsamples of all the stellar sources by defining the following region in the color–color diagram:

$$(H - K) \times 1.97 + 0.54 \geq (J - H) \geq (H - K) \times 1.97 + 0.24,$$

and dividing the stars in that strip at $(H - K) = 0.4$. Stars featuring $(H - K) \geq 0.4$ should be dominated by disk giants with moderate to high extinction, while stars exhibiting $(H - K) < 0.4$ are dominated by nearby disk giants and dwarfs with low extinction. The resolution and extent of these maps allow for a detailed study of Galactic structure which will be the subject of a future work.

5. Conclusions

We have derived empirical transformations from VVV to 2MASS for 152 fields of the VVV survey of the Galactic disk. The transformations in each case have been derived using an iterative clipping algorithm, which improves the robustness of the coefficients. The coefficients reflect the inverse of the relations used in calibrating onto the VISTA photometric system, and as expected we have found statistically significant correlations between the transformation coefficients and the Galactic extinction used in the disk. Our results also suggest some scatter in the transformations which in the case of high extinction fields seem to be related with the inadequacy of the SFD maps used in the zeropoint calibration and require further analysis. Our photometric transformations allow to avoid some of the described uncertainties when working with the VVV catalogues as well as to complement with 2MASS observations when working with saturated objects in the VVV catalogues.

In addition, we presented a stellar CMD and a color–color diagram for 134×10^6 sources in the Galactic plane. The stellar CMD is dominated by main sequence stars in the disk, whose breadth is widened by differential extinction. The sequence tied

to more distant red giants is also seen. In addition, the derived infrared color excess ratio is in agreement with previously reported values. Finally, we present density maps of main sequence stars and red giants. These are useful for identifying overdensities such as star clusters and Galactic spiral arms, as well as the less-populated regions that may correspond to dense clouds.

Acknowledgements. M.S. acknowledges support by Fondecyt project No. 3110188 and Comité Mixto ESO–Chile. We gratefully acknowledge use of data from the ESO Public Survey programme ID 179B-2002 taken with the VISTA telescope, data products from the Cambridge Astronomical Survey Unit, and funding from the FONDAP Center for Astrophysics 15010003, the BASAL CATA Center for Astrophysics and Associated Technologies PFB-06, the MILENO Milky Way Millennium Nucleus from the Ministry of Economy’s ICN grant P07-021-F. R.K.S. and D.M. acknowledge financial support from CONICYT through Gemini Project No. 32080016 and by Proyecto FONDECYT Regular No. 1090213. Support for R.K.S. is provided by the Ministry for the Economy, Development, and Tourism’s Programa Iniciativa Científica Milenio through grant P07-021-F, awarded to The Milky Way Millennium Nucleus. J.B. is supported by FONDECYT No. 1120601. R.K. acknowledges support from Proyecto FONDECYT Regular No. 1130140 and Centro de Astrofísica de Valparaíso. A.R.L. thanks partial financial support from DIULS project CDI12141. RB thanks financial support from FONDECYT Regular No. 1120668. This material is based upon work supported in part by the National Science Foundation under Grant No. 1066293 and the hospitality of the Aspen Center for Physics.

References

- Anderson, J., Sarajedini, A., Bedin, L. R., et al. 2008, AJ, 135, 2055
- Arce, H. G., Goodman, A. A. 1999, ApJ, 517, A264
- Borissova, J., Bonatto, C., Kurtev, R., et al. 2011, A&A, 532, A131
- Bica, E., Bonatto, C., & Camargo, D. 2008, MNRAS, 385, 349
- Binney, J., Gerhard, O. E., Stark, A. A., Bally, J., & Uchida, K. I. 1991, MNRAS, 252, 210
- Binney, J., Gerhard, O. E., & Spergel, D. 1997, MNRAS, 288, 365
- Benjamin, R. A. 2008, ASPC, 387, 375
- Bonifacio, P., Monai, S., & Beers, T. C. 2000, AJ, 120, 2065
- Carpenter, J. M. 2001, AJ, 121, 2851
- Carrao, G., Girardi, L., & Chiosi, C. 1999, MNRAS, 309, 430
- Cuby, J. G., Lidman, C., & Moutou, C. 2000, The Messenger, 101, 2
- Dalton, G. B., Caldwell, M., Ward, A. K., et al. 2006, in SPIE Conf. Ser., 6269
- Emerson, J., McPherson, A., & Sutherland, W. 2006, The Messenger, 126, 41
- Girardi, L., Bressan, A., Bertelli, G., & Chiosi, C. 2000, A&AS, 141, 371
- Girardi, L., Bertelli, G., Bressan, A., et al. 2002, A&A, 391, 195
- Gonzalez, O. A., Rejkuba, M., Zoccali, M., et al. 2012, A&A, 543, A13
- Hodgkin, S. T., Irwin, M. J., Hewett, P. C., & Warren, S. J. 2009, MNRAS, 394, 675
- Indebetouw, R., Mathis, J. S., Babler, B. L., et al. 2005, ApJ, 619, 931
- Irwin, M. J., Lewis, J., Hodgkin, S., et al. 2004, SPIE, 5493, 411
- Kharchenko, N. V., Piskunov, A. E., Röser, S., Schilbach, E., & Scholz, R. D. 2005, A&A, 438, 1163
- Lewis, J. R., Irwin, M., & Buncle, P. 2010, ASPC, 434, 91
- Indebetouw, R., Mathis, J. S., Babler, B. L., et al. 2005, Acta Astron., 60, 55
- Majaess, D. J., Turner, D. G., & Lane, D. J. 2009, MNRAS, 398, 263
- Majaess, D., Moni Bidin, C., et al. 2012, A&A, 537, L4
- Majaess, D., Turner, D. G., Nidever, D. L., et al. 2011, ApJ, 739, 25
- Minniti, D., Lucas, P. W., Emerson, J. P., et al. 2010, New Astron., 15, 433
- Saito, R. K., Hempel, M., Lucas, P. W., et al. 2012, A&A, 537, 107
- Sarajedini, A., Bedin, L. R., Chaboyer, B., et al. 2007, AJ, 133, 1658
- Schlesinger, D. J., Finkbeiner, D. P., & Davis, M. 1998, ApJ, 500, 525
- Skrutskie, M. F., Cutri, R. M., Stiening, R., et al. 2006, AJ, 131, 1163
- Straiž, V. & Laugelys, V. 2008, Balt. Astron., 17, 253

Appendix A: Coefficients of the photometric transformations

Table A.1. Coefficients for the photometric transformations of 152 disk tiles.

Tile	RA (deg)	Dec (deg)	N_{fit}	α_K (mag)	β_K	α_{JH} (mag)	β_{JH}	α_{JK} (mag)	β_{JK}	α_{HK} (mag)	β_{HK}
d001	175.8521	-63.5298	33 644	0.0157 ± 0.0010	-0.0042 ± 0.0008	0.0430 ± 0.0013	0.0693 ± 0.0017	-0.0010 ± 0.0015	0.0446 ± 0.0013	-0.0402 ± 0.0015	-0.0166 ± 0.0038
d002	179.0511	-63.8750	32 106	0.0165 ± 0.0011	-0.0001 ± 0.0011	0.0042 ± 0.0015	0.0860 ± 0.0021	-0.0108 ± 0.0016	0.0545 ± 0.0016	-0.0052 ± 0.0015	-0.0652 ± 0.0048
d003	182.3203	-64.1487	36 215	0.0336 ± 0.0012	-0.0101 ± 0.0012	0.0150 ± 0.0014	0.0926 ± 0.0020	-0.0174 ± 0.0016	0.0642 ± 0.0016	-0.0237 ± 0.0016	-0.0334 ± 0.0054
d004	185.6456	-64.3492	38 982	0.0307 ± 0.0011	-0.0064 ± 0.0011	0.0060 ± 0.0014	0.0968 ± 0.0020	-0.0200 ± 0.0016	0.0611 ± 0.0016	-0.0198 ± 0.0015	-0.0449 ± 0.0051
d005	189.0110	-64.4743	39 338	0.0291 ± 0.0014	0.0031 ± 0.0013	0.0057 ± 0.0017	0.0838 ± 0.0024	-0.0273 ± 0.0019	0.0582 ± 0.0019	-0.0305 ± 0.0020	-0.0122 ± 0.0064
d006	192.3968	-64.5231	36 247	0.0166 ± 0.0014	0.0032 ± 0.0013	0.0205 ± 0.0018	0.0873 ± 0.0024	-0.0159 ± 0.0019	0.0562 ± 0.0018	-0.0296 ± 0.0020	-0.0303 ± 0.0063
d007	195.7848	-64.4954	41 994	0.0411 ± 0.0012	-0.0099 ± 0.0011	0.0171 ± 0.0015	0.0877 ± 0.0021	-0.0242 ± 0.0017	0.0623 ± 0.0016	-0.0361 ± 0.0017	-0.0151 ± 0.0053
d008	199.1573	-64.3908	41 225	0.0499 ± 0.0011	-0.0084 ± 0.0012	0.0039 ± 0.0015	0.0978 ± 0.0022	-0.0320 ± 0.0016	0.0659 ± 0.0017	-0.0279 ± 0.0016	-0.0388 ± 0.0059
d009	202.4951	-64.2108	40 639	0.0648 ± 0.0012	-0.0132 ± 0.0013	-0.0158 ± 0.0016	0.1072 ± 0.0024	-0.0463 ± 0.0017	0.0716 ± 0.0018	-0.0147 ± 0.0017	-0.0900 ± 0.0065
d010	205.7817	-63.9568	39 640	0.0405 ± 0.0011	-0.0092 ± 0.0009	0.0211 ± 0.0015	0.0876 ± 0.0019	-0.0265 ± 0.0016	0.0608 ± 0.0014	-0.0442 ± 0.0015	-0.0116 ± 0.0042
d011	209.0005	-63.6310	37 752	0.0460 ± 0.0010	-0.0105 ± 0.0008	0.0153 ± 0.0014	0.0891 ± 0.0018	-0.0317 ± 0.0015	0.0626 ± 0.0013	-0.0463 ± 0.0014	0.0022 ± 0.0040
d012	212.1401	-63.2358	38 724	0.0451 ± 0.0010	-0.0115 ± 0.0008	0.0209 ± 0.0014	0.0806 ± 0.0017	-0.0338 ± 0.0015	0.0611 ± 0.0012	-0.0505 ± 0.0015	0.0074 ± 0.0037
d013	215.1883	-62.7745	35 996	0.0540 ± 0.0010	-0.0219 ± 0.0009	0.0152 ± 0.0015	0.0960 ± 0.0019	-0.0342 ± 0.0016	0.0697 ± 0.0014	-0.0446 ± 0.0015	-0.0056 ± 0.0042
d014	218.1370	-62.2503	35 191	0.0525 ± 0.0011	-0.0162 ± 0.0010	0.0135 ± 0.0014	0.0966 ± 0.0018	-0.0388 ± 0.0016	0.0718 ± 0.0014	-0.0438 ± 0.0015	-0.0113 ± 0.0043
d015	220.9280	-61.6783	35 629	0.0385 ± 0.0013	-0.0116 ± 0.0012	0.0036 ± 0.0016	0.0957 ± 0.0022	-0.0206 ± 0.0018	0.0604 ± 0.0017	-0.0042 ± 0.0018	-0.0942 ± 0.0055
d016	223.6640	-61.0402	39 461	0.0386 ± 0.0013	-0.0060 ± 0.0011	0.0041 ± 0.0018	0.0928 ± 0.0022	-0.0183 ± 0.0019	0.0571 ± 0.0017	-0.0075 ± 0.0018	-0.0740 ± 0.0052
d017	226.2886	-60.3495	41 024	0.0476 ± 0.0011	-0.0193 ± 0.0009	0.0157 ± 0.0015	0.0916 ± 0.0020	-0.0261 ± 0.0017	0.0641 ± 0.0015	-0.0298 ± 0.0016	-0.0361 ± 0.0045
d018	228.8022	-59.6106	37 765	0.0452 ± 0.0011	-0.0125 ± 0.0008	0.0067 ± 0.0015	0.0795 ± 0.0018	-0.0244 ± 0.0016	0.0610 ± 0.0013	-0.0175 ± 0.0015	-0.0265 ± 0.0040
d019	231.2032	-58.8231	37 859	0.0377 ± 0.0012	-0.0098 ± 0.0010	0.0159 ± 0.0017	0.0743 ± 0.0020	-0.0199 ± 0.0018	0.0566 ± 0.0015	-0.0186 ± 0.0017	-0.0341 ± 0.0046
d020	233.4979	-57.9973	37 687	0.0348 ± 0.0012	-0.0179 ± 0.0009	0.0242 ± 0.0016	0.0828 ± 0.0019	-0.0161 ± 0.0018	0.0617 ± 0.0015	-0.0372 ± 0.0017	0.0073 ± 0.0046
d021	235.6905	-57.1360	30 329	0.0245 ± 0.0012	-0.0084 ± 0.0010	0.0240 ± 0.0018	0.0741 ± 0.0022	0.0017 ± 0.0018	0.0494 ± 0.0015	-0.0132 ± 0.0017	-0.0388 ± 0.0048
d022	237.7803	-56.2361	29 279	0.0324 ± 0.0012	-0.0069 ± 0.0011	0.0239 ± 0.0018	0.0711 ± 0.0024	-0.0049 ± 0.0019	0.0493 ± 0.0017	-0.0260 ± 0.0018	-0.0142 ± 0.0055
d023	239.7733	-55.3031	36 364	0.0396 ± 0.0012	-0.0022 ± 0.0011	0.0145 ± 0.0017	0.0752 ± 0.0022	-0.0204 ± 0.0017	0.0545 ± 0.0016	-0.0243 ± 0.0018	-0.0284 ± 0.0054
d024	241.6744	-54.3403	31 483	0.0422 ± 0.0011	-0.0079 ± 0.0010	0.0313 ± 0.0016	0.0837 ± 0.0022	-0.0199 ± 0.0017	0.0573 ± 0.0016	-0.0401 ± 0.0017	-0.0297 ± 0.0051
d025	243.4888	-53.3495	24 613	0.0691 ± 0.0012	-0.0185 ± 0.0011	0.0022 ± 0.0017	0.0918 ± 0.0023	-0.0417 ± 0.0017	0.0720 ± 0.0017	-0.0380 ± 0.0016	-0.0005 ± 0.0053
d026	245.2210	-52.3332	25 182	0.0829 ± 0.0011	-0.0177 ± 0.0011	-0.0132 ± 0.0017	0.1018 ± 0.0023	-0.0609 ± 0.0017	0.0746 ± 0.0016	-0.0414 ± 0.0017	-0.0196 ± 0.0053
d027	246.8753	-51.2936	19 591	0.0586 ± 0.0014	-0.0069 ± 0.0011	0.0041 ± 0.0023	0.0880 ± 0.0026	-0.0391 ± 0.0023	0.0660 ± 0.0018	-0.0389 ± 0.0022	0.0023 ± 0.0056
d028	248.4570	-50.2325	35 065	0.0411 ± 0.0011	-0.0153 ± 0.0008	0.0346 ± 0.0018	0.0790 ± 0.0020	-0.0137 ± 0.0019	0.0587 ± 0.0014	-0.0397 ± 0.0019	-0.0058 ± 0.0044
d029	249.9705	-49.1513	34 166	0.0437 ± 0.0012	-0.0172 ± 0.0008	0.0455 ± 0.0020	0.0731 ± 0.0020	-0.0050 ± 0.0019	0.0547 ± 0.0014	-0.0446 ± 0.0019	0.0032 ± 0.0042
d030	251.4179	-48.0498	20 597	0.0232 ± 0.0014	-0.0100 ± 0.0011	0.0406 ± 0.0022	0.0738 ± 0.0024	0.0022 ± 0.0022	0.0507 ± 0.0017	-0.0317 ± 0.0023	-0.0231 ± 0.0054
d031	252.8095	-46.9361	32 392	0.0515 ± 0.0011	-0.0076 ± 0.0007	0.0515 ± 0.0017	0.0545 ± 0.0017	-0.0041 ± 0.0018	0.0367 ± 0.0012	-0.0554 ± 0.0018	-0.0035 ± 0.0035
d032	254.1434	-45.8047	19 864	0.0533 ± 0.0014	-0.0150 ± 0.0009	0.0660 ± 0.0023	0.0493 ± 0.0022	-0.0027 ± 0.0023	0.0413 ± 0.0015	-0.0620 ± 0.0023	0.0103 ± 0.0045
d033	255.4246	-44.6591	23 870	0.0445 ± 0.0014	-0.0127 ± 0.0011	0.0254 ± 0.0022	0.0714 ± 0.0025	-0.0213 ± 0.0022	0.0571 ± 0.0017	-0.0323 ± 0.0022	-0.0164 ± 0.0058
d034	256.6573	-43.5002	27 401	0.0207 ± 0.0014	-0.0050 ± 0.0010	0.0447 ± 0.0022	0.0590 ± 0.0023	0.0116 ± 0.0022	0.0384 ± 0.0016	-0.0239 ± 0.0023	-0.0327 ± 0.0051
d035	257.8845	-42.3291	28 967	0.0668 ± 0.0014	-0.0261 ± 0.0010	0.0353 ± 0.0021	0.0690 ± 0.0022	-0.0243 ± 0.0022	0.0597 ± 0.0016	-0.0545 ± 0.0022	0.0283 ± 0.0053
d036	258.9983	-41.1472	22 418	0.0712 ± 0.0016	-0.0176 ± 0.0011	0.0058 ± 0.0024	0.0712 ± 0.0024	-0.0374 ± 0.0025	0.0613 ± 0.0017	-0.0054 ± 0.0024	-0.0595 ± 0.0056
d037	260.0943	-39.9547	25 168	0.0868 ± 0.0015	-0.0174 ± 0.0012	-0.0090 ± 0.0021	0.0946 ± 0.0023	-0.0585 ± 0.0023	0.0789 ± 0.0017	-0.0288 ± 0.0023	-0.0159 ± 0.0056
d038	261.1624	-38.7528	21 461	0.0523 ± 0.0014	-0.0325 ± 0.0010	0.0063 ± 0.0021	0.0937 ± 0.0022	-0.0091 ± 0.0022	0.0741 ± 0.0016	-0.0108 ± 0.0019	0.0095 ± 0.0048
d039	276.4669	-62.4740	26 437	0.0039 ± 0.0011	-0.0030 ± 0.0010	0.0314 ± 0.0015	0.0760 ± 0.0021	0.0041 ± 0.0016	0.0472 ± 0.0015	-0.0259 ± 0.0016	-0.0222 ± 0.0044
d040	279.5577	-62.8066	29 453	0.0339 ± 0.0011	-0.0116 ± 0.0010	0.0293 ± 0.0013	0.0900 ± 0.0019	-0.0238 ± 0.0015	0.0630 ± 0.0015	-0.0497 ± 0.0016	-0.0081 ± 0.0047
d041	282.7113	-63.0705	27 936	0.0278 ± 0.0011	-0.0098 ± 0.0010	0.0100 ± 0.0014	0.0873 ± 0.0019	-0.0109 ± 0.0016	0.0565 ± 0.0015	-0.0191 ± 0.0015	-0.0187 ± 0.0044
d042	285.9145	-63.2635	35 540	0.0325 ± 0.0010	-0.0086 ± 0.0008	0.0284 ± 0.0013	0.0841 ± 0.0016	-0.0164 ± 0.0015	0.0568 ± 0.0012	-0.0430 ± 0.0015	-0.0068 ± 0.0037
d043	289.1504	-63.3840	36 452	0.0348 ± 0.0012	-0.0082 ± 0.0008	0.0342 ± 0.0017	0.0728 ± 0.0018	-0.0167 ± 0.0019	0.0506 ± 0.0013	-0.0501 ± 0.0019	0.0017 ± 0.0039
d044	292.4097	-63.4311	33 496	0.0302 ± 0.0011	-0.0128 ± 0.0008	0.0461 ± 0.0016	0.0801 ± 0.0019	-0.0180 ± 0.0018	<		

Table A.1. continued.

Tile	RA (deg)	DEC (deg)	N_{fit}	α_K (mag)	β_K	α_{JH} (mag)	β_{JH}	α_{JK} (mag)	β_{JK}	α_{HK} (mag)	β_{HK}
d052	217.2655	-61.2391	19 833	0.0305 ± 0.0011	-0.0141 ± 0.0008	0.0596 ± 0.0016	0.0727 ± 0.0019	-0.0161 ± 0.0018	0.0596 ± 0.0013	-0.0717 ± 0.0017	0.0230 ± 0.0036
d053	220.0361	-60.6742	22 541	0.0335 ± 0.0010	-0.0175 ± 0.0007	0.0414 ± 0.0016	0.0797 ± 0.0018	-0.0271 ± 0.0017	0.0619 ± 0.0013	-0.0610 ± 0.0016	0.0095 ± 0.0034
d054	222.7065	-60.0543	28 333	0.0431 ± 0.0010	-0.0192 ± 0.0006	0.0447 ± 0.0017	0.0638 ± 0.0016	-0.0190 ± 0.0018	0.0525 ± 0.0011	-0.0618 ± 0.0017	0.0238 ± 0.0031
d055	225.2751	-59.3830	21 600	0.0387 ± 0.0011	-0.0184 ± 0.0007	0.0622 ± 0.0018	0.0774 ± 0.0018	-0.0120 ± 0.0020	0.0624 ± 0.0013	-0.0719 ± 0.0019	0.0255 ± 0.0035
d056	227.7405	-58.6635	28 631	0.0384 ± 0.0010	-0.0147 ± 0.0006	0.0517 ± 0.0016	0.0730 ± 0.0016	-0.0105 ± 0.0017	0.0589 ± 0.0011	-0.0527 ± 0.0016	0.0119 ± 0.0032
d057	230.1038	-57.8993	20 526	0.0371 ± 0.0014	-0.0148 ± 0.0009	0.0447 ± 0.0021	0.0870 ± 0.0021	-0.0295 ± 0.0023	0.0664 ± 0.0015	-0.0581 ± 0.0023	-0.0038 ± 0.0044
d058	232.3647	-57.0907	28 440	0.0249 ± 0.0012	-0.0167 ± 0.0007	0.0479 ± 0.0019	0.0717 ± 0.0017	-0.0080 ± 0.0021	0.0569 ± 0.0012	-0.0396 ± 0.0020	-0.0004 ± 0.0034
d059	234.5306	-56.2485	23 353	0.0314 ± 0.0012	-0.0106 ± 0.0008	0.0426 ± 0.0020	0.0727 ± 0.0019	0.0057 ± 0.0021	0.0531 ± 0.0013	-0.0311 ± 0.0019	-0.0033 ± 0.0037
d060	236.5999	-55.3681	21 220	0.0528 ± 0.0012	-0.0160 ± 0.0008	0.0389 ± 0.0021	0.0598 ± 0.0020	-0.0191 ± 0.0021	0.0472 ± 0.0013	-0.0550 ± 0.0020	0.0168 ± 0.0038
d061	238.5781	-54.4544	18 196	0.0543 ± 0.0011	-0.0130 ± 0.0007	0.0349 ± 0.0019	0.0572 ± 0.0019	-0.0186 ± 0.0019	0.0475 ± 0.0013	-0.0484 ± 0.0017	0.0142 ± 0.0036
d062	240.4685	-53.5101	9152	0.0540 ± 0.0016	-0.0126 ± 0.0011	0.0507 ± 0.0025	0.0764 ± 0.0026	-0.0258 ± 0.0027	0.0602 ± 0.0018	-0.0702 ± 0.0026	0.0184 ± 0.0052
d063	242.2762	-52.5375	9975	0.0593 ± 0.0016	-0.0200 ± 0.0011	0.0647 ± 0.0024	0.0633 ± 0.0027	-0.0052 ± 0.0026	0.0493 ± 0.0019	-0.0691 ± 0.0025	0.0228 ± 0.0055
d064	244.0048	-51.5388	12 414	0.1223 ± 0.0015	-0.0151 ± 0.0012	-0.0413 ± 0.0023	0.0889 ± 0.0028	-0.1048 ± 0.0023	0.0660 ± 0.0019	-0.0659 ± 0.0022	0.0208 ± 0.0056
d065	245.6584	-50.5163	19 772	0.1118 ± 0.0011	-0.0108 ± 0.0008	0.0077 ± 0.0018	0.0697 ± 0.0021	-0.0836 ± 0.0019	0.0611 ± 0.0014	-0.0874 ± 0.0018	0.0369 ± 0.0039
d066	247.2417	-49.4715	12 612	0.0887 ± 0.0014	-0.0224 ± 0.0009	0.0721 ± 0.0021	0.0725 ± 0.0022	-0.0605 ± 0.0023	0.0705 ± 0.0015	-0.1288 ± 0.0025	0.0566 ± 0.0046
d067	248.7586	-48.4061	4760	0.0556 ± 0.0023	-0.0158 ± 0.0014	0.0601 ± 0.0037	0.0696 ± 0.0036	-0.0444 ± 0.0037	0.0647 ± 0.0024	-0.0935 ± 0.0040	0.0343 ± 0.0074
d068	250.2109	-47.3193	11 065	0.0514 ± 0.0015	-0.0103 ± 0.0010	0.0095 ± 0.0024	0.0579 ± 0.0024	-0.0398 ± 0.0024	0.0500 ± 0.0016	-0.0451 ± 0.0024	0.0239 ± 0.0049
d069	251.6072	-46.2182	12 030	0.0230 ± 0.0013	-0.0135 ± 0.0008	0.0671 ± 0.0020	0.0606 ± 0.0021	0.0031 ± 0.0021	0.0506 ± 0.0014	-0.0581 ± 0.0020	0.0205 ± 0.0040
d070	252.9503	-45.1027	8942	0.4931 ± 0.0023	-0.0048 ± 0.0015	-0.4764 ± 0.0045	0.0450 ± 0.0038	-0.4464 ± 0.0038	0.0425 ± 0.0026	0.0350 ± 0.0020	0.0079 ± 0.0066
d071	254.2399	-43.9703	15 996	0.0514 ± 0.0012	-0.0143 ± 0.0007	0.0692 ± 0.0020	0.0573 ± 0.0019	-0.0144 ± 0.0020	0.0489 ± 0.0013	-0.0769 ± 0.0020	0.0204 ± 0.0037
d072	255.4811	-42.8240	17 456	0.0346 ± 0.0012	-0.0098 ± 0.0008	0.0938 ± 0.0022	0.0406 ± 0.0021	0.0149 ± 0.0022	0.0366 ± 0.0014	-0.0738 ± 0.0021	0.0192 ± 0.0038
d073	256.6775	-41.6650	15 954	0.0776 ± 0.0013	-0.0115 ± 0.0008	0.0361 ± 0.0021	0.0598 ± 0.0022	-0.0596 ± 0.0022	0.0501 ± 0.0015	-0.0872 ± 0.0022	0.0171 ± 0.0042
d074	257.8319	-40.4943	13 721	0.0699 ± 0.0019	-0.0132 ± 0.0012	0.0214 ± 0.0029	0.0737 ± 0.0027	-0.0493 ± 0.0031	0.0581 ± 0.0019	-0.0539 ± 0.0033	-0.0022 ± 0.0061
d075	258.9468	-39.3125	7666	0.0884 ± 0.0025	-0.0105 ± 0.0017	0.0039 ± 0.0034	0.1094 ± 0.0036	-0.0755 ± 0.0038	0.0760 ± 0.0026	-0.0491 ± 0.0041	-0.0564 ± 0.0085
d076	260.0247	-38.1209	5661	0.1482 ± 0.0025	-0.0131 ± 0.0015	-0.1114 ± 0.0037	0.1017 ± 0.0033	-0.1629 ± 0.0040	0.0788 ± 0.0025	-0.0451 ± 0.0036	0.0112 ± 0.0071
d077	177.0402	-61.4155	21 785	0.0166 ± 0.0013	-0.0048 ± 0.0013	0.0090 ± 0.0017	0.0836 ± 0.0025	-0.0096 ± 0.0018	0.0517 ± 0.0019	-0.0098 ± 0.0018	-0.0616 ± 0.0061
d078	180.0302	-61.7369	27 491	0.0223 ± 0.0012	-0.0064 ± 0.0011	0.0005 ± 0.0015	0.0840 ± 0.0021	-0.0162 ± 0.0016	0.0587 ± 0.0016	-0.0066 ± 0.0015	-0.0404 ± 0.0048
d079	183.0765	-61.9914	38 731	0.0403 ± 0.0010	-0.0110 ± 0.0008	0.0220 ± 0.0013	0.0851 ± 0.0016	-0.0223 ± 0.0014	0.0594 ± 0.0013	-0.0411 ± 0.0014	-0.0064 ± 0.0038
d080	186.1673	-62.1775	33 579	0.0238 ± 0.0009	-0.0096 ± 0.0007	0.0280 ± 0.0013	0.0793 ± 0.0017	-0.0119 ± 0.0014	0.0559 ± 0.0012	-0.0381 ± 0.0013	-0.0011 ± 0.0034
d081	189.2895	-62.2934	30 373	0.0324 ± 0.0010	-0.0066 ± 0.0007	0.0427 ± 0.0014	0.0633 ± 0.0016	-0.0051 ± 0.0016	0.0430 ± 0.0011	-0.0455 ± 0.0015	-0.0048 ± 0.0031
d082	192.4280	-62.3390	30 038	0.0384 ± 0.0010	-0.0063 ± 0.0007	0.0635 ± 0.0015	0.0611 ± 0.0017	-0.0160 ± 0.0016	0.0432 ± 0.0012	-0.0724 ± 0.0016	-0.0045 ± 0.0031
d083	195.5693	-62.3131	26 638	-0.0016 ± 0.0010	-0.0112 ± 0.0007	0.0535 ± 0.0015	0.0678 ± 0.0018	-0.0035 ± 0.0017	0.0537 ± 0.0013	-0.0507 ± 0.0015	0.0132 ± 0.0034
d084	198.6969	-62.2164	26 496	0.0611 ± 0.0009	-0.0074 ± 0.0007	-0.0057 ± 0.0015	0.0726 ± 0.0017	-0.0503 ± 0.0015	0.0529 ± 0.0012	-0.0417 ± 0.0013	0.0008 ± 0.0031
d085	201.7978	-62.0493	26 786	0.0218 ± 0.0009	-0.0129 ± 0.0006	0.0375 ± 0.0015	0.0807 ± 0.0016	-0.0185 ± 0.0015	0.0566 ± 0.0011	-0.0532 ± 0.0014	0.0031 ± 0.0031
d086	204.8578	-61.8133	32 466	0.0506 ± 0.0008	-0.0161 ± 0.0006	0.0314 ± 0.0013	0.0853 ± 0.0014	-0.0387 ± 0.0014	0.0653 ± 0.0010	-0.0673 ± 0.0013	0.0196 ± 0.0028
d087	207.8637	-61.5103	26 690	0.0730 ± 0.0009	-0.0158 ± 0.0006	0.0431 ± 0.0014	0.0703 ± 0.0016	-0.0578 ± 0.0016	0.0614 ± 0.0011	-0.0971 ± 0.0015	0.0357 ± 0.0029
d088	210.8059	-61.1419	16 214	-0.0216 ± 0.0012	-0.0051 ± 0.0009	0.0495 ± 0.0019	0.0651 ± 0.0025	0.0105 ± 0.0020	0.0456 ± 0.0017	-0.0367 ± 0.0018	0.0005 ± 0.0042
d089	213.6747	-60.7109	25 868	0.0472 ± 0.0010	-0.0098 ± 0.0006	0.0075 ± 0.0016	0.0652 ± 0.0017	-0.0275 ± 0.0017	0.0480 ± 0.0011	-0.0332 ± 0.0014	0.0058 ± 0.0029
d090	216.4618	-60.2201	24 120	0.0046 ± 0.0010	-0.0086 ± 0.0007	0.0635 ± 0.0015	0.0731 ± 0.0016	0.0105 ± 0.0016	0.0530 ± 0.0012	-0.0511 ± 0.0014	0.0075 ± 0.0030
d091	219.1617	-59.6721	27 827	0.0299 ± 0.0009	-0.0180 ± 0.0006	0.0500 ± 0.0014	0.0742 ± 0.0015	-0.0181 ± 0.0016	0.0607 ± 0.0011	-0.0647 ± 0.0014	0.0252 ± 0.0028
d092	221.7703	-59.0704	23 454	0.0297 ± 0.0011	-0.0134 ± 0.0007	0.0412 ± 0.0018	0.0634 ± 0.0017	0.0024 ± 0.0019	0.0476 ± 0.0012	-0.0367 ± 0.0016	0.0119 ± 0.0032
d093	224.2852	-58.4179	27 588	0.0670 ± 0.0011	-0.0129 ± 0.0007	0.0152 ± 0.0019	0.0691 ± 0.0017	-0.0495 ± 0.0020	0.0523 ± 0.0012	-0.0634 ± 0.0017	0.0152 ± 0.0032
d094	226.7048	-57.7177	28 479	0.0541 ± 0.0011	-0.0147 ± 0.0007	0.0296 ± 0.0017	0.0717 ± 0.0016	-0.0260 ± 0.0018	0.0572 ± 0.0011	-0.0514 ± 0.0017	0.0160 ± 0.0033
d095	229.0299	-56.9725	19 873	0.0636 ± 0.0014	-0.0220 ± 0.0008	0.0372 ± 0.0021	0.0768 ± 0.0019	-0.0345 ± 0.0023	0.0632 ± 0.0014	-0.0620 ± 0.0022	0.0191 ± 0.0039
d096	231.2605	-56.1861	19 845								

Table A.1. continued.

Tile	RA (deg)	Dec (deg)	N_{fit}	α_K (mag)	β_K	α_{JH} (mag)	β_{JH}	α_{JK} (mag)	β_{JK}	α_{HK} (mag)	β_{HK}
d104	246.0499	-48.7074	10 614	0.0410 ± 0.0014	-0.0087 ± 0.0010	0.0500 ± 0.0023	0.0687 ± 0.0026	-0.0245 ± 0.0024	0.0537 ± 0.0018	-0.0711 ± 0.0023	0.0147 ± 0.0049
d105	247.5690	-47.6577	10 570	0.0670 ± 0.0017	-0.0106 ± 0.0011	0.0165 ± 0.0026	0.0737 ± 0.0024	-0.0337 ± 0.0027	0.0518 ± 0.0017	-0.0481 ± 0.0026	0.0028 ± 0.0049
d106	249.0276	-46.5883	9553	0.0836 ± 0.0019	-0.0131 ± 0.0013	0.0238 ± 0.0029	0.0704 ± 0.0029	-0.0512 ± 0.0030	0.0493 ± 0.0020	-0.0745 ± 0.0033	0.0101 ± 0.0065
d107	250.4290	-45.5011	11 628	0.1435 ± 0.0017	-0.0175 ± 0.0011	-0.0354 ± 0.0025	0.0770 ± 0.0026	-0.1061 ± 0.0026	0.0699 ± 0.0018	-0.0703 ± 0.0026	0.0464 ± 0.0057
d108	251.7765	-44.3972	11 346	0.0934 ± 0.0014	-0.0198 ± 0.0010	0.0413 ± 0.0022	0.0747 ± 0.0023	-0.0518 ± 0.0023	0.0623 ± 0.0016	-0.0886 ± 0.0024	0.0301 ± 0.0047
d109	253.0732	-43.2775	14 967	0.0599 ± 0.0013	-0.0134 ± 0.0008	0.0395 ± 0.0020	0.0516 ± 0.0019	-0.0088 ± 0.0021	0.0382 ± 0.0013	-0.0484 ± 0.0020	0.0094 ± 0.0036
d110	254.3225	-42.1437	15 105	0.2776 ± 0.0014	-0.0138 ± 0.0008	-0.1396 ± 0.0025	0.0495 ± 0.0022	-0.2228 ± 0.0025	0.0451 ± 0.0015	-0.0808 ± 0.0021	0.0294 ± 0.0040
d111	255.5272	-40.9968	13 063	0.1743 ± 0.0015	-0.0226 ± 0.0008	-0.0231 ± 0.0025	0.0548 ± 0.0022	-0.1243 ± 0.0026	0.0503 ± 0.0015	-0.0955 ± 0.0023	0.0294 ± 0.0039
d112	256.6880	-39.8348	8893	-0.0144 ± 0.0019	-0.0052 ± 0.0011	0.0465 ± 0.0032	0.0663 ± 0.0028	0.0112 ± 0.0033	0.0404 ± 0.0019	-0.0332 ± 0.0030	-0.0079 ± 0.0051
d113	257.8140	-38.6664	11 314	0.0693 ± 0.0020	-0.0185 ± 0.0011	0.0204 ± 0.0031	0.0734 ± 0.0026	-0.0425 ± 0.0031	0.0609 ± 0.0018	-0.0564 ± 0.0031	0.0236 ± 0.0055
d114	258.9010	-37.4849	8541	0.1028 ± 0.0023	-0.0220 ± 0.0013	-0.0247 ± 0.0035	0.0748 ± 0.0029	-0.0747 ± 0.0036	0.0673 ± 0.0021	-0.0496 ± 0.0034	0.0458 ± 0.0063
d115	177.5766	-60.3547	22 498	0.0016 ± 0.0016	0.0080 ± 0.0020	0.0004 ± 0.0018	0.0805 ± 0.0032	0.0032 ± 0.0020	0.0389 ± 0.0026	0.0190 ± 0.0019	-0.1634 ± 0.0087
d116	180.4729	-60.6657	30 799	0.0244 ± 0.0013	0.0015 ± 0.0014	0.0284 ± 0.0014	0.0890 ± 0.0023	-0.0170 ± 0.0017	0.0523 ± 0.0019	-0.0369 ± 0.0019	-0.0606 ± 0.0065
d117	183.4198	-60.9115	34 255	0.0205 ± 0.0012	-0.0047 ± 0.0012	0.0214 ± 0.0014	0.0793 ± 0.0021	-0.0029 ± 0.0017	0.0451 ± 0.0017	-0.0174 ± 0.0017	-0.0576 ± 0.0057
d118	186.4069	-61.0913	30 502	0.0217 ± 0.0012	-0.0015 ± 0.0014	0.0061 ± 0.0015	0.0907 ± 0.0024	-0.0118 ± 0.0017	0.0505 ± 0.0019	-0.0162 ± 0.0017	-0.0603 ± 0.0065
d119	189.4216	-61.2032	31 512	0.0131 ± 0.0011	0.0009 ± 0.0010	0.0176 ± 0.0015	0.0763 ± 0.0021	0.0014 ± 0.0016	0.0419 ± 0.0016	-0.0161 ± 0.0015	-0.0371 ± 0.0047
d120	192.4518	-61.2469	32 723	0.0322 ± 0.0010	-0.0078 ± 0.0007	0.0315 ± 0.0015	0.0694 ± 0.0018	-0.0089 ± 0.0015	0.0423 ± 0.0013	-0.0402 ± 0.0014	-0.0159 ± 0.0035
d121	195.4831	-61.2217	34 619	0.0428 ± 0.0009	-0.0103 ± 0.0007	0.0298 ± 0.0015	0.0632 ± 0.0016	-0.0105 ± 0.0015	0.0392 ± 0.0011	-0.0414 ± 0.0014	-0.0125 ± 0.0030
d122	198.5034	-61.1281	28 434	0.0157 ± 0.0009	-0.0072 ± 0.0007	0.0394 ± 0.0014	0.0702 ± 0.0017	-0.0026 ± 0.0015	0.0470 ± 0.0012	-0.0402 ± 0.0014	-0.0091 ± 0.0033
d123	201.4990	-60.9663	37 589	0.0283 ± 0.0010	-0.0105 ± 0.0009	0.0184 ± 0.0014	0.0831 ± 0.0019	-0.0091 ± 0.0014	0.0538 ± 0.0013	-0.0282 ± 0.0014	-0.0163 ± 0.0042
d124	204.4580	-60.7383	37 394	0.0238 ± 0.0010	-0.0048 ± 0.0008	0.0341 ± 0.0014	0.0815 ± 0.0017	-0.0053 ± 0.0015	0.0504 ± 0.0013	-0.0371 ± 0.0015	-0.0257 ± 0.0040
d125	207.3688	-60.4448	39 185	0.0454 ± 0.0010	-0.0116 ± 0.0008	0.0176 ± 0.0014	0.0853 ± 0.0016	-0.0284 ± 0.0015	0.0610 ± 0.0012	-0.0441 ± 0.0015	0.0003 ± 0.0038
d126	210.2215	-60.0880	13 152	-0.0243 ± 0.0017	0.0020 ± 0.0015	0.0458 ± 0.0026	0.0631 ± 0.0034	0.0377 ± 0.0026	0.0315 ± 0.0024	-0.0057 ± 0.0025	-0.0427 ± 0.0070
d127	213.0073	-59.6704	34 969	0.0251 ± 0.0011	-0.0095 ± 0.0009	0.0436 ± 0.0016	0.0755 ± 0.0018	-0.0045 ± 0.0017	0.0507 ± 0.0013	-0.0427 ± 0.0016	-0.0104 ± 0.0039
d128	215.7194	-59.1940	36 971	0.0258 ± 0.0012	-0.0104 ± 0.0009	0.0379 ± 0.0016	0.0749 ± 0.0018	-0.0083 ± 0.0017	0.0525 ± 0.0013	-0.0397 ± 0.0017	-0.0078 ± 0.0041
d129	218.3517	-58.6620	38 828	0.0355 ± 0.0012	-0.0096 ± 0.0010	0.0244 ± 0.0016	0.0811 ± 0.0019	-0.0182 ± 0.0017	0.0558 ± 0.0014	-0.0358 ± 0.0017	-0.0202 ± 0.0044
d130	220.9005	-58.0769	42 793	0.0437 ± 0.0012	-0.0046 ± 0.0010	0.0234 ± 0.0016	0.0693 ± 0.0020	-0.0119 ± 0.0018	0.0471 ± 0.0015	-0.0295 ± 0.0017	-0.0290 ± 0.0050
d131	223.3630	-57.4416	39 251	0.0322 ± 0.0014	-0.0081 ± 0.0011	0.0369 ± 0.0018	0.0686 ± 0.0021	-0.0144 ± 0.0020	0.0543 ± 0.0016	-0.0428 ± 0.0020	0.0015 ± 0.0051
d132	225.7375	-56.7590	38 041	0.0205 ± 0.0013	0.0010 ± 0.0009	0.0369 ± 0.0017	0.0657 ± 0.0019	0.0039 ± 0.0019	0.0422 ± 0.0014	-0.0226 ± 0.0018	-0.0338 ± 0.0044
d133	228.0234	-56.0321	37 301	0.0290 ± 0.0011	-0.0052 ± 0.0008	0.0400 ± 0.0017	0.0652 ± 0.0017	-0.0059 ± 0.0018	0.0466 ± 0.0013	-0.0472 ± 0.0017	0.0083 ± 0.0036
d134	230.2212	-55.2638	35 123	0.0405 ± 0.0012	-0.0027 ± 0.0009	0.0329 ± 0.0017	0.0663 ± 0.0019	-0.0180 ± 0.0019	0.0528 ± 0.0014	-0.0472 ± 0.0019	0.0090 ± 0.0045
d135	232.3327	-54.4564	38 429	0.0360 ± 0.0011	-0.0055 ± 0.0008	0.0289 ± 0.0016	0.0668 ± 0.0017	-0.0160 ± 0.0017	0.0494 ± 0.0013	-0.0416 ± 0.0016	0.0000 ± 0.0036
d136	234.3604	-53.6129	27 647	0.0491 ± 0.0012	-0.0090 ± 0.0009	0.0183 ± 0.0019	0.0724 ± 0.0019	-0.0219 ± 0.0019	0.0530 ± 0.0014	-0.0381 ± 0.0018	-0.0007 ± 0.0042
d137	236.3054	-52.7358	23 251	0.0462 ± 0.0012	-0.0130 ± 0.0008	0.0283 ± 0.0019	0.0758 ± 0.0020	-0.0208 ± 0.0019	0.0561 ± 0.0014	-0.0456 ± 0.0018	0.0032 ± 0.0039
d138	238.1700	-51.8245	24 966	0.0294 ± 0.0011	-0.0100 ± 0.0007	0.0390 ± 0.0019	0.0675 ± 0.0019	-0.0118 ± 0.0019	0.0485 ± 0.0013	-0.0487 ± 0.0017	0.0038 ± 0.0034
d139	239.9601	-50.8868	25 817	0.0380 ± 0.0011	-0.0127 ± 0.0008	0.0131 ± 0.0018	0.0774 ± 0.0018	-0.0228 ± 0.0019	0.0575 ± 0.0013	-0.0298 ± 0.0016	-0.0053 ± 0.0036
d140	241.6791	-49.9245	13 848	0.0073 ± 0.0016	-0.0047 ± 0.0011	0.0792 ± 0.0026	0.0483 ± 0.0026	0.0467 ± 0.0027	0.0262 ± 0.0018	-0.0255 ± 0.0025	-0.0342 ± 0.0052
d141	243.3271	-48.9346	27 439	0.0465 ± 0.0011	-0.0169 ± 0.0007	0.0415 ± 0.0018	0.0572 ± 0.0017	0.0004 ± 0.0018	0.0450 ± 0.0012	-0.0396 ± 0.0017	0.0115 ± 0.0035
d142	244.9090	-47.9215	29 181	0.0514 ± 0.0012	-0.0089 ± 0.0009	0.0064 ± 0.0019	0.0677 ± 0.0021	-0.0179 ± 0.0019	0.0480 ± 0.0014	-0.0130 ± 0.0018	-0.0339 ± 0.0045
d143	246.4288	-46.8865	13 081	0.0382 ± 0.0021	-0.0019 ± 0.0018	0.0084 ± 0.0030	0.0793 ± 0.0035	-0.0081 ± 0.0032	0.0457 ± 0.0027	-0.0088 ± 0.0029	-0.0625 ± 0.0085
d144	247.8894	-45.8315	33 916	0.0479 ± 0.0014	-0.0124 ± 0.0012	0.0325 ± 0.0020	0.0735 ± 0.0023	-0.0048 ± 0.0021	0.0485 ± 0.0017	-0.0259 ± 0.0022	-0.0442 ± 0.0058
d145	249.2940	-44.7579	32 141	0.0409 ± 0.0014	-0.0096 ± 0.0012	0.0301 ± 0.0020	0.0718 ± 0.0023	-0.0067 ± 0.0021	0.0498 ± 0.0017	-0.0318 ± 0.0022	-0.0186 ± 0.0059
d146	250.6457	-43.6672	28 503	0.0201 ± 0.0013	-0.0112 ± 0.0009	0.0356 ± 0.0019	0.0734 ± 0.0020	0.0032 ± 0.0019	0.0573 ± 0.0014	-0.0219 ± 0.0019	-0.0057 ± 0.0046
d147	251.9480	-42.5603	21 646	0.0319 ± 0.0014	-0.0084 ± 0.0010	0.0576 ± 0.0021	0.0656 ± 0.0022	0.0017 ± 0.0022	0.0421 ± 0.0016	-0.0450 ± 0.0023	-0.0307 ± 0.0051

Appendix B: Coefficients of the photometric transformations separated by populations

In addition to the transformations presented in the previous section, we have produced similar coefficients discriminating the different stellar populations with a simple procedure. Figure B.1 illustrates the technique: for each field we calculated a color histogram for a range of colors, where a double Gaussian fit is used to estimate the minimum between the main sequence and post-main sequence star distributions. This minimum is then used as limit to separate both populations in the CMD. Tables B.1 and B.2 show the derived coefficients of the photometric transformations for main sequence, and post main sequence stars respectively, which have been calculated using the same procedure applied to the complete sample.

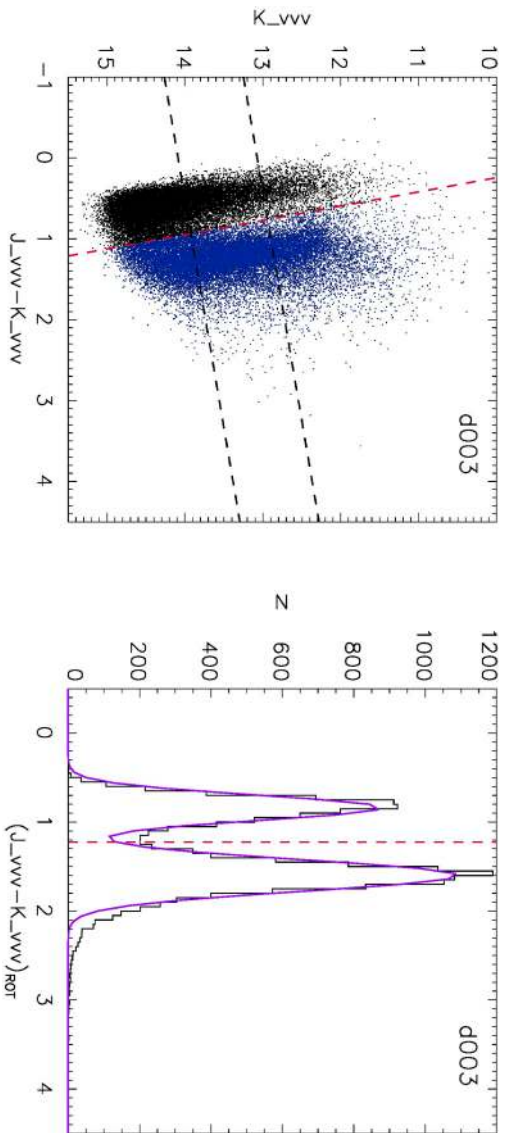


Fig. B.1. Example of the procedure applied to separate the stellar populations in each tile. *Left*, CMD for the VVV tile $d003$, the subsample of stars between the black dashed lines has been chosen to calculate an histogram of the color equation $(J-K)_{\text{rot}} = (J-K+1.0) \times 0.983 - (10.0-K) \times 0.174$. *Right*, respective histogram for the stars selected in the CMD, a double Gaussian fitting (solid purple line) is used estimate the minimum between the main sequence and post main sequence distributions (red dashed line), which is used to separate the populations.

Table B.1. Coefficients for the photometric transformations of 152 disk tiles divided by population: main sequence stars.

Tile	RA (deg)	Dec (deg)	N_{fit}	α_K (mag)	β_K	α_{JH} (mag)	β_{JH}	α_{JK} (mag)	β_{JK}	α_{HK} (mag)	β_{HK}
d001	175.8521	-63.5298	20 830	0.0244 ± 0.0024	-0.0180 ± 0.0033	0.0438 ± 0.0025	0.0653 ± 0.0053	-0.0108 ± 0.0030	0.0597 ± 0.0042	-0.0454 ± 0.0032	0.0103 ± 0.0127
d002	179.0511	-63.8750	18 636	0.0266 ± 0.0027	-0.0137 ± 0.0042	0.0149 ± 0.0028	0.0512 ± 0.0062	-0.0231 ± 0.0034	0.0756 ± 0.0053	-0.0152 ± 0.0031	0.0001 ± 0.0160
d003	182.3203	-64.1487	19 237	0.0394 ± 0.0029	-0.0178 ± 0.0045	0.0251 ± 0.0029	0.0619 ± 0.0067	-0.0280 ± 0.0036	0.0832 ± 0.0056	-0.0323 ± 0.0035	0.0208 ± 0.0169
d004	185.6456	-64.3492	18 036	0.0238 ± 0.0032	0.0070 ± 0.0051	0.0222 ± 0.0032	0.0505 ± 0.0074	-0.0217 ± 0.0040	0.0649 ± 0.0065	-0.0289 ± 0.0037	0.0204 ± 0.0194
d005	189.0110	-64.4743	18 075	0.0349 ± 0.0036	0.0001 ± 0.0051	0.0126 ± 0.0037	0.0602 ± 0.0075	-0.0396 ± 0.0046	0.0747 ± 0.0065	-0.0336 ± 0.0048	0.0220 ± 0.0214
d006	192.3968	-64.5231	16 958	0.0088 ± 0.0035	0.0208 ± 0.0049	0.0271 ± 0.0037	0.0698 ± 0.0077	-0.0290 ± 0.0044	0.0771 ± 0.0063	-0.0372 ± 0.0046	0.0159 ± 0.0196
d007	195.7848	-64.4954	19 198	0.0451 ± 0.0032	-0.0130 ± 0.0046	0.0229 ± 0.0033	0.0675 ± 0.0070	-0.0395 ± 0.0041	0.0881 ± 0.0060	-0.0417 ± 0.0041	0.0319 ± 0.0187
d008	199.1573	-64.3908	20 041	0.0403 ± 0.0029	0.0152 ± 0.0046	0.0128 ± 0.0031	0.0703 ± 0.0069	-0.0385 ± 0.0038	0.0756 ± 0.0059	-0.0302 ± 0.0039	-0.0205 ± 0.0201
d009	202.4951	-64.2108	18 073	0.0580 ± 0.0032	0.0040 ± 0.0054	0.0046 ± 0.0034	0.0451 ± 0.0080	-0.0562 ± 0.0043	0.0866 ± 0.0071	-0.0208 ± 0.0043	-0.0539 ± 0.0248
d010	205.7817	-63.9568	16 316	0.0315 ± 0.0031	0.0102 ± 0.0045	0.0240 ± 0.0035	0.0773 ± 0.0075	-0.0329 ± 0.0040	0.0679 ± 0.0058	-0.0418 ± 0.0037	-0.0256 ± 0.0160
d011	209.0005	-63.6310	18 461	0.0469 ± 0.0030	-0.0072 ± 0.0043	0.0208 ± 0.0033	0.0698 ± 0.0070	-0.0444 ± 0.0039	0.0798 ± 0.0056	-0.0440 ± 0.0039	-0.0002 ± 0.0172
d012	212.1401	-63.2358	21 203	0.0365 ± 0.0024	0.0030 ± 0.0030	0.0275 ± 0.0027	0.0642 ± 0.0052	-0.0384 ± 0.0032	0.0670 ± 0.0041	-0.0456 ± 0.0033	-0.0141 ± 0.0126
d013	215.1883	-62.7745	17 065	0.0439 ± 0.0033	-0.0070 ± 0.0046	0.0316 ± 0.0036	0.0560 ± 0.0075	-0.0431 ± 0.0043	0.0844 ± 0.0060	-0.0383 ± 0.0041	-0.0304 ± 0.0176
d014	218.1370	-62.2503	17 145	0.0404 ± 0.0031	0.0050 ± 0.0044	0.0296 ± 0.0031	0.0549 ± 0.0065	-0.0404 ± 0.0040	0.0725 ± 0.0057	-0.0366 ± 0.0038	-0.0438 ± 0.0174
d015	220.9280	-61.6783	15 270	0.0153 ± 0.0042	0.0266 ± 0.0062	0.0220 ± 0.0043	0.0532 ± 0.0092	-0.0113 ± 0.0054	0.0448 ± 0.0080	0.0219 ± 0.0048	-0.2394 ± 0.0224
d016	223.6640	-61.0402	20 048	0.0216 ± 0.0034	0.0197 ± 0.0041	0.0230 ± 0.0036	0.0512 ± 0.0062	-0.0202 ± 0.0045	0.0595 ± 0.0054	0.0097 ± 0.0045	-0.1415 ± 0.0177
d017	226.2886	-60.3495	18 348	0.0196 ± 0.0036	0.0215 ± 0.0049	0.0351 ± 0.0037	0.0465 ± 0.0074	-0.0204 ± 0.0047	0.0560 ± 0.0065	0.0022 ± 0.0045	-0.1786 ± 0.0195
d018	228.8022	-59.6106	18 876	0.0204 ± 0.0031	0.0242 ± 0.0038	0.0340 ± 0.0034	0.0190 ± 0.0061	-0.0202 ± 0.0041	0.0532 ± 0.0051	0.0136 ± 0.0036	-0.1656 ± 0.0146
d019	231.2032	-58.8231	17 027	0.0277 ± 0.0036	0.0064 ± 0.0046	0.0383 ± 0.0039	0.0215 ± 0.0072	-0.0189 ± 0.0048	0.0525 ± 0.0060	-0.0211 ± 0.0045	-0.1024 ± 0.0180
d020	233.4979	-57.9973	16 820	0.0149 ± 0.0034	0.0088 ± 0.0043	0.0336 ± 0.0037	0.0604 ± 0.0069	-0.0174 ± 0.0045	0.0629 ± 0.0057	-0.0250 ± 0.0046	-0.0369 ± 0.0176
d021	235.6905	-57.1360	13 403	0.0079 ± 0.0043	0.0169 ± 0.0058	0.0483 ± 0.0048	0.0174 ± 0.0094	-0.0039 ± 0.0056	0.0572 ± 0.0076	0.0103 ± 0.0055	-0.1454 ± 0.0242
d022	237.7803	-56.2361	12 632	0.0164 ± 0.0040	0.0233 ± 0.0057	0.0406 ± 0.0044	0.0268 ± 0.0090	0.0053 ± 0.0053	0.0299 ± 0.0076	-0.0065 ± 0.0051	-0.1049 ± 0.0243
d023	239.7733	-55.3031	15 203	0.0224 ± 0.0042	0.0309 ± 0.0060	0.0367 ± 0.0045	0.0187 ± 0.0092	-0.0112 ± 0.0055	0.0368 ± 0.0079	0.0030 ± 0.0056	-0.1595 ± 0.0265
d024	241.6744	-54.3403	13 609	0.0422 ± 0.0036	-0.0012 ± 0.0055	0.0241 ± 0.0040	0.1004 ± 0.0090	-0.0339 ± 0.0048	0.0772 ± 0.0074	-0.0170 ± 0.0052	-0.1555 ± 0.0244
d025	243.4888	-53.3495	10 327	0.0558 ± 0.0037	0.0130 ± 0.0064	0.0121 ± 0.0042	0.0612 ± 0.0103	-0.0461 ± 0.0049	0.0781 ± 0.0086	-0.0232 ± 0.0048	-0.0978 ± 0.0298
d026	245.2210	-52.3332	12 480	0.0690 ± 0.0026	0.0101 ± 0.0040	-0.0083 ± 0.0032	0.0871 ± 0.0071	-0.0585 ± 0.0036	0.0680 ± 0.0056	-0.0204 ± 0.0039	-0.1484 ± 0.0204
d027	246.8753	-51.2936	7789	0.0209 ± 0.0047	0.0499 ± 0.0061	0.0231 ± 0.0059	0.0429 ± 0.0113	-0.0279 ± 0.0064	0.0483 ± 0.0084	-0.0294 ± 0.0061	-0.0374 ± 0.0254
d028	248.4570	-50.2325	13 818	0.0180 ± 0.0037	0.0138 ± 0.0043	0.0547 ± 0.0048	0.0385 ± 0.0083	-0.0009 ± 0.0052	0.0418 ± 0.0060	-0.0201 ± 0.0055	-0.0768 ± 0.0190
d029	249.9705	-49.1513	13 167	0.0304 ± 0.0034	-0.0003 ± 0.0036	0.0441 ± 0.0045	0.0701 ± 0.0072	-0.0173 ± 0.0047	0.0670 ± 0.0051	-0.0433 ± 0.0050	0.0030 ± 0.0159
d030	251.4179	-48.0498	8616	-0.0030 ± 0.0041	0.0245 ± 0.0051	0.0606 ± 0.0048	0.0300 ± 0.0089	0.0047 ± 0.0055	0.0453 ± 0.0069	-0.0154 ± 0.0062	-0.0903 ± 0.0236
d031	252.8095	-46.9361	12 576	0.0248 ± 0.0038	0.0259 ± 0.0041	0.0641 ± 0.0044	0.0277 ± 0.0072	-0.0003 ± 0.0051	0.0283 ± 0.0056	-0.0356 ± 0.0055	-0.0715 ± 0.0174
d032	254.1434	-45.8047	7981	0.0521 ± 0.0040	-0.0138 ± 0.0041	0.0667 ± 0.0050	0.0448 ± 0.0078	-0.0199 ± 0.0054	0.0578 ± 0.0055	-0.0662 ± 0.0057	0.0228 ± 0.0167
d033	255.4246	-44.6591	9294	0.0547 ± 0.0037	-0.0241 ± 0.0047	0.0420 ± 0.0045	0.0329 ± 0.0084	-0.0283 ± 0.0050	0.0644 ± 0.0065	-0.0368 ± 0.0058	-0.0001 ± 0.0238
d034	256.6573	-43.5002	9330	0.0100 ± 0.0050	0.0107 ± 0.0058	0.0650 ± 0.0064	0.0156 ± 0.0109	0.0046 ± 0.0069	0.0429 ± 0.0079	-0.0131 ± 0.0066	-0.0772 ± 0.0231
d035	257.8445	-42.3291	10 270	0.0565 ± 0.0044	-0.0174 ± 0.0051	0.0564 ± 0.0054	0.0219 ± 0.0093	-0.0333 ± 0.0060	0.0709 ± 0.0070	-0.0439 ± 0.0058	0.0022 ± 0.0205
d036	258.9893	-41.1472	7661	0.0433 ± 0.0046	0.0114 ± 0.0050	0.0590 ± 0.0056	-0.0274 ± 0.0090	-0.0428 ± 0.0064	0.0653 ± 0.0070	0.0378 ± 0.0053	-0.2416 ± 0.0181
d037	260.0943	-39.9547	8029	0.0517 ± 0.0051	0.0280 ± 0.0063	0.0447 ± 0.0053	-0.0158 ± 0.0097	-0.0617 ± 0.0068	0.0797 ± 0.0085	-0.0129 ± 0.0062	-0.0919 ± 0.0237
d038	261.1624	-38.7528	5850	0.0141 ± 0.0051	0.0161 ± 0.0070	0.0459 ± 0.0058	0.0050 ± 0.0114	-0.0150 ± 0.0068	0.0801 ± 0.0095	0.0228 ± 0.0057	-0.1543 ± 0.0265
d039	267.4669	-62.4740	16 882	0.0148 ± 0.0026	-0.0230 ± 0.0039	0.0309 ± 0.0028	0.0730 ± 0.0065	-0.0060 ± 0.0033	0.0648 ± 0.0051	-0.0312 ± 0.0034	0.0136 ± 0.0150
d040	179.5577	-62.8066	17 663	0.0345 ± 0.0025	-0.0101 ± 0.0040	0.0281 ± 0.0025	0.0899 ± 0.0061	-0.0364 ± 0.0032	0.0848 ± 0.0051	-0.0539 ± 0.0033	0.0154 ± 0.0149
d041	182.7113	-63.0705	16 352	0.0223 ± 0.0027	0.0015 ± 0.0041	0.0153 ± 0.0030	0.0692 ± 0.0066	-0.0149 ± 0.0035	0.0616 ± 0.0053	-0.0159 ± 0.0032	-0.0253 ± 0.0151
d042	185.9145	-63.2635	18 063	0.0324 ± 0.0025	-0.0036 ± 0.0035	0.0354 ± 0.0028	0.0600 ± 0.0059	-0.0219 ± 0.0033	0.0608 ± 0.0045	-0.0469 ± 0.0030	0.0207 ± 0.0118
d043	189.1504	-63.3840	16 314	0.0320 ± 0.0034	-0.0022 ± 0.0037	0.0459 ± 0.0039	0.0459 ± 0.0066	-0.0240 ± 0.0044	0.0563 ± 0.0048	-0.0514 ± 0.0042	0.0094 ± 0.0129
d044	192.4097	-63.4311	17 272	0.0129 ± 0.0034	0.0113 ± 0.0040	0.0465 ± 0.0037	0.0749 ± 0.0070	-0.0241 ± 0.0044	0.0645 ± 0.0053	-0.0596 ± 0.0047	0.0091 ± 0.0150
d045	195.6688	-63.4045	16 076	0.0242 ± 0.0034	-0.0058 ± 0.0040	0.0513 ± 0.0039	0.0656 ± 0.0073	-0.0321 ± 0.0045	0.0658 ± 0.0053	-0.0599 ± 0.0044	-0.0116 ± 0.0142
d046	198.9137	-63.3040	16 366	0.0544 ± 0.0028	0.0061 ± 0.0036	0.0054 ± 0.0032	0.0887 ± 0.0063	-0.0510 ± 0.0036	0.0721 ± 0.0047	-0.0460 ± 0.0036	-0.0080 ± 0.0139
d047	202.1286	-63.1310	10 416	0.0598 ± 0.0038	0.0057 ± 0.0059	0.0011 ± 0.0046	0.0657 ± 0.0105	-0.0610 ± 0.0050	0.0770 ± 0.0079	-0.0308 ± 0.0044	-0.0485 ± 0.0214
d048	205.2976	-62.8863	15 340	0.0438 ± 0.0026	-0.0056 ± 0.0031	0.0440 ± 0.0031	0.0650 ± 0.0058	-0.0431 ± 0.0034	0.0675 ± 0.0041	-0.0732 ± 0.0033	0.0210 ± 0.0109
d049	208.4062	-62.5724	16 605	0.0652 ± 0.0022	-0.0101 ± 0.0024	0.0651 ± 0.0024	0.0743 ± 0.0045	-0.0783 ± 0.0029	0.0716 ± 0.0032	-0.1330 ± 0.0033	0.0408 ± 0.0088
d050	211.4437	-62.1913	18 826	0.0294 ± 0.0020	-0.0058 ± 0.0022	0.0531 ± 0.0024	0.0731 ± 0.0043	-0.0203 ± 0.0027	0.0641 ± 0.0030	-0.0587 ± 0.0027	-0.0035 ± 0.0083
d051	214.3995	-61.7459	19 634	0.0365 ± 0.0023	0.0037 ± 0.0023	0.0423 ± 0.0027	0.0587 ± 0.0044	-0.0376 ± 0.0030	0.0540 ± 0.0031	-0.0631 ± 0.0029	-0.0044 ± 0.0083
d052	217.2655	-61.2391	12 973	0.0124 ± 0.0027	0.0087 ± 0.0033	0.0677 ± 0.0030	0.0524 ± 0.0057	-0.0200 ± 0.0035	0.0628 ± 0.0043	-0.0706 ± 0.0035	0.0188 ± 0.0117

Table B.1. continued.

Tile	RA (deg)	Dec (deg)	N_{fit}	α_K (mag)	β_K	α_{JH} (mag)	β_{JH}	α_{JK} (mag)	β_{JK}	α_{HK} (mag)	β_{HK}
d053	220.0361	-60.6742	13 793	0.0235 ± 0.0030	-0.0067 ± 0.0037	0.0458 ± 0.0032	0.0685 ± 0.0063	-0.0288 ± 0.0039	0.0631 ± 0.0049	-0.0518 ± 0.0038	-0.0256 ± 0.0133
d054	222.7065	-60.0543	15 469	0.0310 ± 0.0033	-0.0085 ± 0.0033	0.0479 ± 0.0039	0.0572 ± 0.0061	-0.0368 ± 0.0044	0.0713 ± 0.0044	-0.0601 ± 0.0042	0.0200 ± 0.0117
d055	225.2751	-59.3830	12 846	0.0110 ± 0.0032	0.0096 ± 0.0031	0.0712 ± 0.0039	0.0590 ± 0.0060	-0.0142 ± 0.0044	0.0626 ± 0.0044	-0.0648 ± 0.0044	0.0071 ± 0.0119
d056	227.7405	-58.6635	16 729	0.0150 ± 0.0028	0.0116 ± 0.0029	0.0611 ± 0.0035	0.0541 ± 0.0055	-0.0116 ± 0.0039	0.0582 ± 0.0040	-0.0440 ± 0.0037	-0.0148 ± 0.0107
d057	230.1038	-57.8993	10 619	0.0238 ± 0.0042	0.0000 ± 0.0042	0.0480 ± 0.0051	0.0788 ± 0.0082	-0.0407 ± 0.0058	0.0778 ± 0.0059	-0.0488 ± 0.0057	-0.0335 ± 0.0156
d058	232.3647	-57.0907	13 859	0.0033 ± 0.0032	0.0032 ± 0.0029	0.0568 ± 0.0042	0.0558 ± 0.0058	-0.0146 ± 0.0045	0.0628 ± 0.0040	-0.0341 ± 0.0042	-0.0161 ± 0.0106
d059	234.5306	-56.2485	12 161	0.0201 ± 0.0030	0.0022 ± 0.0028	0.0456 ± 0.0040	0.0657 ± 0.0059	0.0042 ± 0.0041	0.0546 ± 0.0040	-0.0288 ± 0.0039	-0.0089 ± 0.0108
d060	236.5999	-55.3681	11 352	0.0332 ± 0.0036	0.0032 ± 0.0036	0.0425 ± 0.0047	0.0502 ± 0.0072	-0.0318 ± 0.0049	0.0596 ± 0.0048	-0.0498 ± 0.0047	0.0043 ± 0.0130
d061	238.5781	-54.4544	9975	0.0434 ± 0.0037	-0.0007 ± 0.0045	0.0354 ± 0.0044	0.0537 ± 0.0080	-0.0176 ± 0.0049	0.0444 ± 0.0060	-0.0371 ± 0.0046	-0.0305 ± 0.0168
d062	240.4685	-53.5101	5023	0.0475 ± 0.0040	-0.0060 ± 0.0046	0.0479 ± 0.0048	0.0814 ± 0.0087	-0.0343 ± 0.0054	0.0717 ± 0.0062	-0.0610 ± 0.0057	-0.0098 ± 0.0182
d063	242.2762	-52.5375	5072	0.0615 ± 0.0047	-0.0240 ± 0.0060	0.0534 ± 0.0054	0.0851 ± 0.0110	-0.0168 ± 0.0064	0.0636 ± 0.0083	-0.0701 ± 0.0069	0.0314 ± 0.0247
d064	244.0048	-51.5388	7291	0.1271 ± 0.0038	-0.0197 ± 0.0049	-0.0295 ± 0.0046	0.0615 ± 0.0088	-0.1160 ± 0.0051	0.0789 ± 0.0066	-0.0661 ± 0.0048	0.0177 ± 0.0189
d065	245.6584	-50.5163	14 598	0.1079 ± 0.0024	-0.0069 ± 0.0024	0.0069 ± 0.0030	0.0706 ± 0.0048	-0.0838 ± 0.0032	0.0608 ± 0.0033	-0.0849 ± 0.0033	0.0285 ± 0.0098
d066	247.2417	-49.4715	7436	0.0777 ± 0.0032	-0.0098 ± 0.0036	0.0828 ± 0.0036	0.0493 ± 0.0066	-0.0644 ± 0.0044	0.0753 ± 0.0049	-0.1195 ± 0.0054	0.0286 ± 0.0149
d067	248.7586	-48.4061	2206	0.0793 ± 0.0074	-0.0463 ± 0.0090	0.0683 ± 0.0087	0.0512 ± 0.0173	-0.0643 ± 0.0107	0.0884 ± 0.0133	-0.1277 ± 0.0118	0.1427 ± 0.0377
d068	250.2109	-47.3193	5598	0.0457 ± 0.0041	-0.0033 ± 0.0050	0.0142 ± 0.0050	0.0436 ± 0.0092	-0.0506 ± 0.0054	0.0615 ± 0.0067	-0.0373 ± 0.0051	-0.0060 ± 0.0194
d069	251.6072	-46.2182	7703	0.0239 ± 0.0028	-0.0155 ± 0.0032	0.0552 ± 0.0033	0.0813 ± 0.0058	-0.0178 ± 0.0037	0.0758 ± 0.0042	-0.0500 ± 0.0037	-0.0058 ± 0.0118
d070	252.9503	-45.1027	8274	0.4905 ± 0.0035	-0.0023 ± 0.0026	-0.4758 ± 0.0058	0.0445 ± 0.0053	-0.4524 ± 0.0050	0.0477 ± 0.0038	0.0379 ± 0.0025	-0.0094 ± 0.0105
d071	254.2399	-43.9703	8138	0.0478 ± 0.0031	-0.0107 ± 0.0034	0.0675 ± 0.0037	0.0584 ± 0.0064	-0.0298 ± 0.0040	0.0665 ± 0.0044	-0.0808 ± 0.0043	0.0321 ± 0.0127
d072	255.4811	-42.8240	12 494	0.0216 ± 0.0027	0.0021 ± 0.0023	0.0819 ± 0.0036	0.0583 ± 0.0050	0.0062 ± 0.0038	0.0451 ± 0.0033	-0.0653 ± 0.0037	-0.0034 ± 0.0086
d073	256.6775	-41.6650	10 337	0.0730 ± 0.0036	-0.0083 ± 0.0037	0.0379 ± 0.0043	0.0548 ± 0.0070	-0.0715 ± 0.0048	0.0624 ± 0.0050	-0.0896 ± 0.0052	0.0244 ± 0.0146
d074	257.8319	-40.4943	5619	0.0644 ± 0.0055	-0.0097 ± 0.0052	0.0366 ± 0.0068	0.0424 ± 0.0101	-0.0427 ± 0.0077	0.0500 ± 0.0074	-0.0105 ± 0.0078	-0.1254 ± 0.0210
d075	258.9468	-39.3125	3389	0.0939 ± 0.0069	-0.0172 ± 0.0077	0.0324 ± 0.0076	0.0561 ± 0.0135	-0.0690 ± 0.0094	0.0676 ± 0.0106	0.0049 ± 0.0093	-0.2455 ± 0.0278
d076	260.0247	-38.1209	2691	0.1516 ± 0.0070	-0.0169 ± 0.0074	-0.0894 ± 0.0084	0.0578 ± 0.0130	-0.1709 ± 0.0093	0.0854 ± 0.0101	-0.0125 ± 0.0075	-0.1077 ± 0.0259
d077	177.0402	-61.4155	14200	0.0154 ± 0.0028	-0.0059 ± 0.0046	0.0226 ± 0.0029	0.0414 ± 0.0068	-0.0139 ± 0.0036	0.0595 ± 0.0060	-0.0017 ± 0.0039	-0.1045 ± 0.0210
d078	180.0302	-61.7369	16 290	0.0255 ± 0.0027	-0.0090 ± 0.0042	0.0114 ± 0.0028	0.0489 ± 0.0064	-0.0215 ± 0.0034	0.0669 ± 0.0054	-0.0050 ± 0.0029	-0.0498 ± 0.0160
d079	183.0765	-61.9914	22 195	0.0403 ± 0.0025	-0.0084 ± 0.0036	0.0282 ± 0.0026	0.0670 ± 0.0057	-0.0284 ± 0.0032	0.0678 ± 0.0047	-0.0426 ± 0.0030	0.0041 ± 0.0127
d080	186.1673	-62.1775	22 666	0.0223 ± 0.0021	-0.0067 ± 0.0028	0.0368 ± 0.0023	0.0557 ± 0.0047	-0.0182 ± 0.0027	0.0653 ± 0.0037	-0.0422 ± 0.0027	0.0248 ± 0.0114
d081	189.2895	-62.2934	19 906	0.0308 ± 0.0024	-0.0035 ± 0.0027	0.0481 ± 0.0027	0.0511 ± 0.0049	-0.0123 ± 0.0031	0.0519 ± 0.0036	-0.0500 ± 0.0031	0.0128 ± 0.0101
d082	192.4280	-62.3390	20 767	0.0329 ± 0.0027	0.0004 ± 0.0028	0.0616 ± 0.0030	0.0635 ± 0.0052	-0.0245 ± 0.0035	0.0524 ± 0.0038	-0.0693 ± 0.0039	-0.0164 ± 0.0110
d083	195.5693	-62.3131	20 111	-0.0006 ± 0.0025	-0.0125 ± 0.0028	0.0576 ± 0.0029	0.0585 ± 0.0048	-0.0178 ± 0.0034	0.0713 ± 0.0038	-0.0576 ± 0.0036	0.0372 ± 0.0116
d084	198.6969	-62.2164	19 581	0.0540 ± 0.0023	0.0034 ± 0.0027	-0.0014 ± 0.0027	0.0631 ± 0.0046	-0.0498 ± 0.0030	0.0508 ± 0.0036	-0.0373 ± 0.0029	-0.0202 ± 0.0108
d085	201.7978	-62.0493	15 466	0.0133 ± 0.0022	-0.0033 ± 0.0028	0.0370 ± 0.0028	0.0782 ± 0.0053	-0.0257 ± 0.0030	0.0645 ± 0.0037	-0.0517 ± 0.0030	-0.0019 ± 0.0107
d086	204.8578	-61.8133	18 682	0.0426 ± 0.0022	-0.0038 ± 0.0027	0.0325 ± 0.0026	0.0811 ± 0.0049	-0.0423 ± 0.0029	0.0679 ± 0.0036	-0.0616 ± 0.0030	-0.0090 ± 0.0103
d087	207.8637	-61.5103	19 576	0.0644 ± 0.0019	-0.0052 ± 0.0021	0.0455 ± 0.0023	0.0643 ± 0.0039	-0.0594 ± 0.0026	0.0627 ± 0.0028	-0.0967 ± 0.0027	0.0336 ± 0.0078
d088	210.8059	-61.1419	13 816	-0.0253 ± 0.0022	-0.0006 ± 0.0024	0.0468 ± 0.0029	0.0704 ± 0.0049	0.0072 ± 0.0031	0.0491 ± 0.0034	-0.0341 ± 0.0030	-0.0096 ± 0.0094
d089	213.6747	-60.7109	18 618	0.0428 ± 0.0021	-0.0046 ± 0.0021	0.0123 ± 0.0027	0.0548 ± 0.0040	-0.0343 ± 0.0029	0.0550 ± 0.0028	-0.0346 ± 0.0025	0.0103 ± 0.0076
d090	216.4618	-60.2201	15 320	0.0003 ± 0.0024	-0.0045 ± 0.0029	0.0638 ± 0.0028	0.0713 ± 0.0052	0.0052 ± 0.0031	0.0597 ± 0.0038	-0.0549 ± 0.0030	0.0238 ± 0.0102
d091	219.1617	-59.6721	16 255	0.0191 ± 0.0025	-0.0044 ± 0.0030	0.0606 ± 0.0029	0.0495 ± 0.0054	-0.0180 ± 0.0034	0.0581 ± 0.0041	-0.0608 ± 0.0032	0.0057 ± 0.0111
d092	221.7703	-59.0704	12 417	0.0145 ± 0.0030	0.0022 ± 0.0033	0.0503 ± 0.0038	0.0433 ± 0.0061	-0.0024 ± 0.0041	0.0514 ± 0.0044	-0.0288 ± 0.0036	-0.0122 ± 0.0121
d093	224.2852	-58.4179	11 727	0.0523 ± 0.0040	0.0048 ± 0.0041	0.0210 ± 0.0049	0.0538 ± 0.0076	-0.0582 ± 0.0053	0.0561 ± 0.0055	-0.0622 ± 0.0047	0.0084 ± 0.0140
d094	226.7048	-57.7177	14 275	0.0333 ± 0.0027	0.0088 ± 0.0026	0.0462 ± 0.0035	0.0409 ± 0.0051	-0.0257 ± 0.0037	0.0552 ± 0.0035	-0.0532 ± 0.0035	0.0209 ± 0.0095
d095	229.0299	-56.9725	9826	0.0403 ± 0.0032	0.0020 ± 0.0030	0.0452 ± 0.0041	0.0614 ± 0.0060	-0.0374 ± 0.0044	0.0648 ± 0.0041	-0.0634 ± 0.0043	0.0235 ± 0.0111
d096	231.2605	-56.1861	8544	0.0358 ± 0.0041	0.0125 ± 0.0040	0.0726 ± 0.0049	0.0048 ± 0.0074	-0.0234 ± 0.0054	0.0457 ± 0.0053	-0.0639 ± 0.0051	0.0235 ± 0.0140
d097	233.3992	-5									

Table B.1. continued.

Tile	RA (deg)	Dec (deg)	N_{fit}	α_K (mag)	β_K	α_{JH} (mag)	β_{JH}	α_{JK} (mag)	β_{JK}	α_{HK} (mag)	β_{HK}
d107	250.4290	-45.5011	7268	0.1518 ± 0.0032	-0.0258 ± 0.0032	-0.0355 ± 0.0041	0.0761 ± 0.0061	-0.1207 ± 0.0044	0.0854 ± 0.0044	-0.0631 ± 0.0045	0.0168 ± 0.0143
d108	251.7765	-44.3972	7251	0.0920 ± 0.0032	-0.0169 ± 0.0035	0.0433 ± 0.0038	0.0692 ± 0.0066	-0.0515 ± 0.0043	0.0614 ± 0.0048	-0.0809 ± 0.0047	0.0049 ± 0.0142
d109	253.0732	-43.2775	9146	0.0488 ± 0.0027	0.0000 ± 0.0026	0.0333 ± 0.0035	0.0600 ± 0.0053	-0.0196 ± 0.0036	0.0485 ± 0.0036	-0.0491 ± 0.0035	0.0092 ± 0.0099
d110	254.3225	-42.1437	11455	0.2634 ± 0.0029	-0.0011 ± 0.0022	-0.1439 ± 0.0040	0.0545 ± 0.0046	-0.2265 ± 0.0039	0.0478 ± 0.0031	-0.0784 ± 0.0035	0.0208 ± 0.0087
d111	255.5272	-40.9968	9155	0.1562 ± 0.0029	-0.0066 ± 0.0023	-0.0290 ± 0.0039	0.0623 ± 0.0047	-0.1230 ± 0.0040	0.0485 ± 0.0032	-0.0896 ± 0.0038	0.0132 ± 0.0086
d112	256.6880	-39.8348	5488	-0.0142 ± 0.0038	-0.0063 ± 0.0032	0.0359 ± 0.0050	0.0815 ± 0.0067	-0.0070 ± 0.0052	0.0576 ± 0.0045	-0.0352 ± 0.0050	-0.0016 ± 0.0123
d113	257.8140	-38.6664	4328	0.0531 ± 0.0048	-0.0046 ± 0.0045	0.0262 ± 0.0061	0.0602 ± 0.0089	-0.0470 ± 0.0062	0.0645 ± 0.0059	-0.0550 ± 0.0059	0.0228 ± 0.0164
d114	258.9010	-37.4849	2185	0.0829 ± 0.0081	0.0004 ± 0.0093	0.0024 ± 0.0100	0.0214 ± 0.0168	-0.0840 ± 0.0106	0.0717 ± 0.0124	-0.0288 ± 0.0083	-0.0328 ± 0.0314
d115	177.5766	-60.3547	13382	0.0339 ± 0.0040	-0.0645 ± 0.0075	0.0092 ± 0.0038	0.0494 ± 0.0096	-0.0354 ± 0.0050	0.1222 ± 0.0094	0.0138 ± 0.0048	-0.1231 ± 0.0341
d116	180.4729	-60.6657	17186	0.0421 ± 0.0037	-0.0305 ± 0.0064	0.0361 ± 0.0031	0.0625 ± 0.0082	-0.0357 ± 0.0045	0.0884 ± 0.0078	-0.0365 ± 0.0053	-0.0554 ± 0.0273
d117	183.4198	-60.9115	18927	0.0331 ± 0.0034	-0.0279 ± 0.0054	0.0302 ± 0.0033	0.0518 ± 0.0075	-0.0196 ± 0.0043	0.0721 ± 0.0068	-0.0196 ± 0.0043	-0.0372 ± 0.0218
d118	186.4069	-61.0913	16417	0.0400 ± 0.0038	-0.0362 ± 0.0068	0.0258 ± 0.0035	0.0280 ± 0.0087	-0.0310 ± 0.0047	0.0854 ± 0.0084	-0.0326 ± 0.0052	0.0625 ± 0.0311
d119	189.4216	-61.2032	19057	0.0237 ± 0.0028	-0.0168 ± 0.0042	0.0205 ± 0.0028	0.0634 ± 0.0060	-0.0154 ± 0.0035	0.0671 ± 0.0053	-0.0158 ± 0.0037	-0.0244 ± 0.0191
d120	192.4518	-61.2469	18977	0.0344 ± 0.0028	-0.0117 ± 0.0036	0.0294 ± 0.0029	0.0721 ± 0.0057	-0.0161 ± 0.0035	0.0509 ± 0.0046	-0.0368 ± 0.0036	-0.0299 ± 0.0141
d121	195.4831	-61.2217	19125	0.0498 ± 0.0027	-0.0197 ± 0.0032	0.0330 ± 0.0029	0.0527 ± 0.0051	-0.0216 ± 0.0035	0.0516 ± 0.0041	-0.0348 ± 0.0034	-0.0366 ± 0.0122
d122	198.5034	-61.1281	18095	0.0193 ± 0.0027	-0.0128 ± 0.0036	0.0399 ± 0.0029	0.0670 ± 0.0057	-0.0206 ± 0.0035	0.0724 ± 0.0047	-0.0430 ± 0.0036	0.0036 ± 0.0150
d123	201.4990	-60.9663	19317	0.0191 ± 0.0028	0.0043 ± 0.0042	0.0197 ± 0.0030	0.0709 ± 0.0064	-0.0256 ± 0.0036	0.0776 ± 0.0054	-0.0304 ± 0.0036	0.0105 ± 0.0182
d124	204.4580	-60.7383	18930	0.0179 ± 0.0027	0.0070 ± 0.0038	0.0377 ± 0.0030	0.0679 ± 0.0062	-0.0086 ± 0.0036	0.0500 ± 0.0051	-0.0357 ± 0.0036	-0.0406 ± 0.0157
d125	207.3688	-60.4448	19130	0.0375 ± 0.0029	0.0019 ± 0.0040	0.0242 ± 0.0032	0.0652 ± 0.0064	-0.0403 ± 0.0038	0.0764 ± 0.0052	-0.0458 ± 0.0036	0.0153 ± 0.0153
d126	210.2215	-60.0880	8064	-0.0291 ± 0.0042	0.0059 ± 0.0060	0.0502 ± 0.0051	0.0522 ± 0.0106	0.0274 ± 0.0055	0.0493 ± 0.0079	-0.0018 ± 0.0051	-0.0595 ± 0.0237
d127	213.0073	-59.6704	16629	0.0206 ± 0.0028	-0.0013 ± 0.0035	0.0477 ± 0.0032	0.0648 ± 0.0060	-0.0164 ± 0.0036	0.0667 ± 0.0045	-0.0520 ± 0.0035	0.0296 ± 0.0129
d128	215.7194	-59.1940	17805	0.0272 ± 0.0030	-0.0131 ± 0.0037	0.0430 ± 0.0033	0.0606 ± 0.0062	-0.0189 ± 0.0039	0.0664 ± 0.0048	-0.0431 ± 0.0036	0.0103 ± 0.0136
d129	218.3517	-58.6620	18277	0.0340 ± 0.0033	-0.0075 ± 0.0043	0.0346 ± 0.0036	0.0565 ± 0.0069	-0.0301 ± 0.0043	0.0713 ± 0.0056	-0.0337 ± 0.0041	-0.0290 ± 0.0165
d130	220.9005	-58.0769	19276	0.0251 ± 0.0033	0.0254 ± 0.0043	0.0448 ± 0.0037	0.0179 ± 0.0069	-0.0199 ± 0.0043	0.0541 ± 0.0056	-0.0378 ± 0.0042	0.0159 ± 0.0178
d131	223.3630	-57.4416	19099	0.0250 ± 0.0032	0.0036 ± 0.0036	0.0353 ± 0.0037	0.0690 ± 0.0061	-0.0279 ± 0.0044	0.0698 ± 0.0049	-0.0486 ± 0.0043	0.0224 ± 0.0147
d132	225.7375	-56.7590	17539	0.0130 ± 0.0031	0.0147 ± 0.0034	0.0409 ± 0.0038	0.0503 ± 0.0060	-0.0143 ± 0.0042	0.0597 ± 0.0045	-0.0290 ± 0.0038	-0.0113 ± 0.0126
d133	228.0234	-56.0321	15989	0.0175 ± 0.0031	0.0134 ± 0.0034	0.0514 ± 0.0039	0.0367 ± 0.0063	-0.0207 ± 0.0042	0.0596 ± 0.0045	-0.0516 ± 0.0039	0.0292 ± 0.0126
d134	230.2212	-55.2638	12705	0.0169 ± 0.0043	0.0362 ± 0.0054	0.0727 ± 0.0048	-0.0281 ± 0.0088	-0.0200 ± 0.0056	0.0473 ± 0.0070	-0.0413 ± 0.0051	-0.0129 ± 0.0193
d135	232.3327	-54.4564	15951	0.0260 ± 0.0034	0.0101 ± 0.0040	0.0348 ± 0.0038	0.0474 ± 0.0066	-0.0260 ± 0.0044	0.0584 ± 0.0053	-0.0322 ± 0.0040	-0.0255 ± 0.0148
d136	234.3604	-53.6129	10819	0.0288 ± 0.0037	0.0240 ± 0.0044	0.0447 ± 0.0044	0.0106 ± 0.0078	-0.0296 ± 0.0049	0.0567 ± 0.0058	-0.0359 ± 0.0043	-0.0071 ± 0.0160
d137	236.3054	-52.7358	11454	0.0209 ± 0.0033	0.0210 ± 0.0036	0.0451 ± 0.0042	0.0406 ± 0.0070	-0.0213 ± 0.0044	0.0533 ± 0.0048	-0.0454 ± 0.0042	-0.0003 ± 0.0136
d138	238.1700	-51.8245	14391	0.0153 ± 0.0029	0.0070 ± 0.0029	0.0468 ± 0.0040	0.0512 ± 0.0060	-0.0167 ± 0.0040	0.0534 ± 0.0040	-0.0451 ± 0.0038	-0.0066 ± 0.0111
d139	239.9601	-50.8868	13527	0.0043 ± 0.0037	0.0292 ± 0.0040	0.0506 ± 0.0044	0.0102 ± 0.0070	-0.0223 ± 0.0050	0.0559 ± 0.0055	-0.0165 ± 0.0044	-0.0531 ± 0.0151
d140	241.6791	-49.9245	7318	0.0030 ± 0.0044	0.0039 ± 0.0047	0.0907 ± 0.0058	0.0257 ± 0.0095	0.0368 ± 0.0061	0.0350 ± 0.0066	-0.0312 ± 0.0059	-0.0165 ± 0.0188
d141	243.3271	-48.9346	11930	0.0137 ± 0.0032	0.0202 ± 0.0035	0.0520 ± 0.0043	0.0340 ± 0.0068	-0.0021 ± 0.0044	0.0467 ± 0.0048	-0.0255 ± 0.0041	-0.0411 ± 0.0139
d142	244.9090	-47.9215	11834	0.0110 ± 0.0045	0.0487 ± 0.0057	0.0427 ± 0.0052	-0.0074 ± 0.0092	-0.0094 ± 0.0060	0.0333 ± 0.0075	0.0018 ± 0.0055	-0.1096 ± 0.0233
d143	246.4288	-46.8865	5015	0.0226 ± 0.0063	0.0268 ± 0.0082	0.0163 ± 0.0074	0.0593 ± 0.0134	-0.0243 ± 0.0085	0.0628 ± 0.0112	0.0054 ± 0.0077	-0.1502 ± 0.0358
d144	247.8894	-45.8315	11050	0.0080 ± 0.0047	0.0418 ± 0.0061	0.0529 ± 0.0053	0.0277 ± 0.0100	-0.0095 ± 0.0063	0.0534 ± 0.0081	-0.0249 ± 0.0061	-0.0504 ± 0.0245
d145	249.2940	-44.7579	11143	0.0331 ± 0.0041	0.0066 ± 0.0053	0.0347 ± 0.0048	0.0536 ± 0.0090	-0.0251 ± 0.0056	0.0684 ± 0.0071	-0.0312 ± 0.0059	-0.0205 ± 0.0236
d146	250.6457	-43.6672	10135	0.0357 ± 0.0040	-0.0270 ± 0.0050	0.0381 ± 0.0048	0.0625 ± 0.0088	-0.0209 ± 0.0053	0.0832 ± 0.0066	-0.0293 ± 0.0052	0.0105 ± 0.0201
d147	251.9480	-42.5603	8633	0.0311 ± 0.0040	-0.0052 ± 0.0047	0.0622 ± 0.0050	0.0534 ± 0.0090	-0.0178 ± 0.0056	0.0624 ± 0.0066	-0.0570 ± 0.0056	-0.0013 ± 0.0197
d148	253.2033	-41.4384	2796	0.0516 ± 0.0080	-0.0250 ± 0.0110	0.0378 ± 0.0099	0.0658 ± 0.0202	-0.0149 ± 0.0109	0.0513 ± 0.0151	-0.0368 ± 0.0105	-0.0385 ± 0.0446
d149	254.4150	-40.3029	7277	0.0239 ± 0.0045	-0.0007 ± 0.0055	0.0476 ± 0.0054	0.0600 ± 0.0099	-0.0161 ± 0.0059	0.0700 ± 0.0073	-0.0527 ± 0.0055	0.0356 ± 0.0213
d150	255.5831	-39.1525	5915	0.0174 ± 0.0048	-0.0234 ± 0.0060	0.0644 ± 0.0062	0.0384 ± 0.0114	-0.0078 ± 0.0064	0.0804 ± 0.0080	-0.0434 ± 0.0055	0.0435 ± 0.0213

Table B.2. Coefficients for the photometric transformations of 152 disk tiles divided by population: post main sequence stars.

Tile	RA (deg)	Dec (deg)	N_{fit}	α_K (mag)	β_K	α_{JH} (mag)	β_{JH}	α_{JK} (mag)	β_{JK}	α_{HK} (mag)	β_{HK}
d001	175.8521	-63.5298	12 814	0.0147 ± 0.0032	-0.0032 ± 0.0019	0.0623 ± 0.0058	0.0524 ± 0.0052	0.0172 ± 0.0057	0.0331 ± 0.0034	-0.0483 ± 0.0045	-0.0026 ± 0.0082
d002	179.0511	-63.8750	13 469	-0.0129 ± 0.0033	0.0202 ± 0.0024	0.1162 ± 0.0053	-0.0265 ± 0.0055	0.0211 ± 0.0056	0.0309 ± 0.0041	-0.0050 ± 0.0043	-0.0669 ± 0.0102
d003	182.3203	-64.1487	16 978	0.0118 ± 0.0034	0.0063 ± 0.0026	0.0456 ± 0.0054	0.0595 ± 0.0060	-0.0047 ± 0.0053	0.0542 ± 0.0041	-0.0271 ± 0.0042	-0.0262 ± 0.0109
d004	185.6456	-64.3492	20 946	0.0286 ± 0.0025	-0.0050 ± 0.0020	0.0131 ± 0.0040	0.0901 ± 0.0045	-0.0229 ± 0.0039	0.0633 ± 0.0031	-0.0306 ± 0.0031	-0.0195 ± 0.0083
d005	189.0110	-64.4743	21 262	-0.0054 ± 0.0029	0.0291 ± 0.0023	0.0574 ± 0.0046	0.0264 ± 0.0053	-0.0071 ± 0.0046	0.0419 ± 0.0037	-0.0518 ± 0.0038	0.0405 ± 0.0103
d006	192.3968	-64.5231	19 288	-0.0143 ± 0.0032	0.0261 ± 0.0025	0.0327 ± 0.0052	0.0740 ± 0.0059	-0.0114 ± 0.0049	0.0523 ± 0.0039	-0.0417 ± 0.0042	-0.0021 ± 0.0108
d007	195.7848	-64.4954	22 795	0.0225 ± 0.0026	0.0038 ± 0.0021	0.0603 ± 0.0045	0.0404 ± 0.0051	-0.0257 ± 0.0043	0.0629 ± 0.0034	-0.0564 ± 0.0035	0.0336 ± 0.0091
d008	199.1573	-64.3908	21 183	0.0095 ± 0.0027	0.0237 ± 0.0023	0.0417 ± 0.0048	0.0539 ± 0.0057	-0.0145 ± 0.0043	0.0511 ± 0.0037	-0.0361 ± 0.0034	-0.0164 ± 0.0100
d009	202.4951	-64.2108	22 566	0.0320 ± 0.0031	0.0148 ± 0.0027	0.0534 ± 0.0049	0.0241 ± 0.0062	-0.0250 ± 0.0048	0.0526 ± 0.0043	-0.0127 ± 0.0038	-0.0952 ± 0.0121
d010	205.7817	-63.9568	23 323	0.0279 ± 0.0019	-0.0012 ± 0.0014	0.0330 ± 0.0035	0.0757 ± 0.0037	-0.0110 ± 0.0033	0.0500 ± 0.0024	-0.0422 ± 0.0027	-0.0155 ± 0.0063
d011	209.0005	-63.6310	19 290	0.0302 ± 0.0020	-0.0006 ± 0.0014	0.0447 ± 0.0038	0.0608 ± 0.0038	-0.0154 ± 0.0036	0.0516 ± 0.0025	-0.0542 ± 0.0029	0.0174 ± 0.0063
d012	212.1401	-63.2358	17 520	0.0258 ± 0.0029	-0.0004 ± 0.0017	0.0463 ± 0.0057	0.0593 ± 0.0050	-0.0167 ± 0.0054	0.0505 ± 0.0033	-0.0541 ± 0.0043	0.0135 ± 0.0082
d013	215.1883	-62.7745	18 930	0.0543 ± 0.0024	-0.0223 ± 0.0016	0.0288 ± 0.0043	0.0837 ± 0.0043	-0.0413 ± 0.0040	0.0743 ± 0.0028	-0.0515 ± 0.0033	0.0091 ± 0.0072
d014	218.1370	-62.2503	18 045	0.0360 ± 0.0026	-0.0058 ± 0.0018	0.0472 ± 0.0045	0.0643 ± 0.0046	-0.0202 ± 0.0044	0.0591 ± 0.0031	-0.0493 ± 0.0033	0.0006 ± 0.0076
d015	220.9280	-61.6783	20 359	0.0350 ± 0.0026	-0.0092 ± 0.0021	0.0005 ± 0.0043	0.1002 ± 0.0048	-0.0179 ± 0.0041	0.0583 ± 0.0033	0.0049 ± 0.0033	-0.1138 ± 0.0086
d016	223.6640	-61.0402	19 412	0.0178 ± 0.0027	0.0074 ± 0.0019	0.0418 ± 0.0049	0.0568 ± 0.0050	-0.0130 ± 0.0045	0.0533 ± 0.0033	-0.0191 ± 0.0035	-0.0468 ± 0.0083
d017	226.2886	-60.3495	22 675	0.0494 ± 0.0021	-0.0208 ± 0.0015	0.0228 ± 0.0036	0.0855 ± 0.0038	-0.0297 ± 0.0034	0.0666 ± 0.0025	-0.0389 ± 0.0028	-0.0152 ± 0.0067
d018	228.8022	-59.6106	18 889	0.0281 ± 0.0024	-0.0028 ± 0.0016	0.0858 ± 0.0044	0.0114 ± 0.0041	-0.0063 ± 0.0044	0.0499 ± 0.0029	-0.0216 ± 0.0034	-0.0162 ± 0.0071
d019	231.2032	-58.8231	20 832	0.0248 ± 0.0023	-0.0023 ± 0.0016	0.0617 ± 0.0039	0.0322 ± 0.0039	-0.0036 ± 0.0039	0.0461 ± 0.0027	-0.0258 ± 0.0032	-0.0176 ± 0.0074
d020	233.4979	-57.9973	20 866	0.0392 ± 0.0024	-0.0208 ± 0.0016	0.0462 ± 0.0041	0.0619 ± 0.0040	-0.0158 ± 0.0040	0.0610 ± 0.0027	-0.0517 ± 0.0034	0.0368 ± 0.0074
d021	235.6905	-57.1360	16 925	0.0210 ± 0.0023	-0.0064 ± 0.0016	0.0457 ± 0.0043	0.0551 ± 0.0042	0.0007 ± 0.0039	0.0500 ± 0.0027	-0.0198 ± 0.0032	-0.0243 ± 0.0073
d022	237.7803	-56.2361	16 646	0.0165 ± 0.0023	0.0037 ± 0.0017	0.0490 ± 0.0042	0.0461 ± 0.0046	0.0064 ± 0.0039	0.0415 ± 0.0029	-0.0329 ± 0.0031	0.0031 ± 0.0080
d023	239.7733	-55.3031	21 160	0.0064 ± 0.0025	0.0208 ± 0.0019	0.0575 ± 0.0045	0.0319 ± 0.0048	0.0023 ± 0.0042	0.0382 ± 0.0031	-0.0301 ± 0.0035	-0.0134 ± 0.0090
d024	241.6744	-54.3403	17 873	0.0104 ± 0.0026	0.0142 ± 0.0019	0.0392 ± 0.0046	0.0752 ± 0.0050	-0.0025 ± 0.0043	0.0446 ± 0.0032	-0.0294 ± 0.0035	-0.0531 ± 0.0087
d025	243.4888	-53.3495	14 285	0.0431 ± 0.0026	0.0001 ± 0.0021	0.0249 ± 0.0047	0.0678 ± 0.0051	-0.0277 ± 0.0044	0.0612 ± 0.0034	-0.0404 ± 0.0033	0.0057 ± 0.0090
d026	245.2210	-52.3332	12 702	0.0558 ± 0.0033	0.0006 ± 0.0024	0.0144 ± 0.0063	0.0739 ± 0.0066	-0.0446 ± 0.0058	0.0634 ± 0.0043	-0.0340 ± 0.0047	-0.0347 ± 0.0115
d027	246.8753	-51.2936	11 801	0.0393 ± 0.0029	0.0044 ± 0.0019	0.0365 ± 0.0056	0.0588 ± 0.0053	-0.0242 ± 0.0051	0.0565 ± 0.0034	-0.0463 ± 0.0042	0.0168 ± 0.0091
d028	248.4570	-50.2325	21 246	0.0335 ± 0.0023	-0.0111 ± 0.0015	0.0529 ± 0.0046	0.0633 ± 0.0042	-0.0020 ± 0.0042	0.0515 ± 0.0027	-0.0432 ± 0.0035	0.0017 ± 0.0070
d029	249.9705	-49.1513	20 998	0.0361 ± 0.0022	-0.0130 ± 0.0014	0.0728 ± 0.0046	0.0494 ± 0.0041	0.0107 ± 0.0042	0.0452 ± 0.0026	-0.0501 ± 0.0034	0.0129 ± 0.0065
d030	251.4179	-48.0498	11 980	0.0284 ± 0.0034	-0.0134 ± 0.0021	0.0720 ± 0.0065	0.0464 ± 0.0059	0.0259 ± 0.0062	0.0363 ± 0.0039	-0.0298 ± 0.0049	-0.0258 ± 0.0098
d031	252.8095	-46.9361	19 815	0.0406 ± 0.0022	-0.0023 ± 0.0012	0.0886 ± 0.0044	0.0254 ± 0.0036	0.0324 ± 0.0042	0.0175 ± 0.0023	-0.0548 ± 0.0035	-0.0032 ± 0.0059
d032	254.1434	-45.8047	11 883	0.0555 ± 0.0029	-0.0163 ± 0.0015	0.0968 ± 0.0061	0.0261 ± 0.0048	0.0264 ± 0.0059	0.0260 ± 0.0032	-0.0619 ± 0.0046	0.0102 ± 0.0077
d033	255.4246	-44.6591	14 575	0.0290 ± 0.0033	-0.0029 ± 0.0022	0.0483 ± 0.0063	0.0509 ± 0.0061	-0.0039 ± 0.0058	0.0457 ± 0.0039	-0.0239 ± 0.0049	-0.0345 ± 0.0109
d034	256.6573	-43.5002	18 070	0.0065 ± 0.0029	0.0030 ± 0.0018	0.0856 ± 0.0054	0.0240 ± 0.0048	0.0467 ± 0.0051	0.0177 ± 0.0031	-0.0183 ± 0.0044	-0.0430 ± 0.0088
d035	257.8445	-42.3291	18 697	0.0891 ± 0.0029	-0.0394 ± 0.0018	0.0789 ± 0.0053	0.0307 ± 0.0049	-0.0238 ± 0.0051	0.0589 ± 0.0033	-0.0795 ± 0.0044	0.0778 ± 0.0092
d036	258.9893	-41.1472	14 756	0.0904 ± 0.0035	-0.0292 ± 0.0021	0.0927 ± 0.0062	-0.0017 ± 0.0055	-0.0018 ± 0.0061	0.0402 ± 0.0038	0.0199 ± 0.0048	-0.1048 ± 0.0098
d037	260.0943	-39.9547	17 138	0.0930 ± 0.0034	-0.0215 ± 0.0022	0.0323 ± 0.0059	0.0580 ± 0.0055	-0.0318 ± 0.0059	0.0618 ± 0.0039	-0.0140 ± 0.0044	-0.0463 ± 0.0097
d038	261.1624	-38.7528	15 610	0.0656 ± 0.0022	-0.0406 ± 0.0015	0.0263 ± 0.0044	0.0760 ± 0.0041	-0.0005 ± 0.0041	0.0687 ± 0.0027	-0.0158 ± 0.0029	0.0209 ± 0.0065
d039	267.4669	-62.4740	9554	0.0056 ± 0.0032	-0.0034 ± 0.0020	0.0776 ± 0.0063	0.0331 ± 0.0059	0.0159 ± 0.0060	0.0392 ± 0.0038	-0.0455 ± 0.0046	0.0138 ± 0.0091
d040	179.5577	-62.8066	11 789	0.0170 ± 0.0034	-0.0007 ± 0.0024	0.0674 ± 0.0062	0.0511 ± 0.0063	0.0019 ± 0.0060	0.0445 ± 0.0042	-0.0513 ± 0.0047	-0.0048 ± 0.0101
d041	182.7113	-63.0705	11 583	0.0175 ± 0.0030	-0.0036 ± 0.0020	0.0603 ± 0.0055	0.0400 ± 0.0053	-0.0005 ± 0.0053	0.0495 ± 0.0035	-0.0409 ± 0.0042	0.0261 ± 0.0090
d042	185.9145	-63.2635	17 476	0.0099 ± 0.0026	0.0046 ± 0.0016	0.0811 ± 0.0047	0.0363 ± 0.0044	0.0185 ± 0.0047	0.0352 ± 0.0030	-0.0592 ± 0.0038	0.0238 ± 0.0074
d043	189.1504	-63.3840	20 138	0.0159 ± 0.0027	0.0018 ± 0.0015	0.0686 ± 0.0050	0.0440 ± 0.0043	0.0157 ± 0.0050	0.0323 ± 0.0029	-0.0543 ± 0.0041	0.0089 ± 0.0072
d044	192.4097	-63.4311	16 223	0.0213 ± 0.0024	-0.0084 ± 0.0014	0.0806 ± 0.0049	0.0495 ± 0.0044	0.0012 ± 0.0046	0.0471 ± 0.0028	-0.0727 ± 0.0038	0.0290 ± 0.0069
d045	195.6688	-63.4045	16 500	0.0254 ± 0.0022	-0.0125 ± 0.0013	0.0549 ± 0.0045	0.0709 ± 0.0039	-0.0152 ± 0.0043	0.0512 ± 0.0025	-0.0553 ± 0.0034	-0.0174 ± 0.0060
d046	198.9137	-63.3040	14 661	0.0713 ± 0.0022	-0.0201 ± 0.0013	0.0331 ± 0.0044	0.0680 ± 0.0040	-0.0429 ± 0.0042	0.0669 ± 0.0026	-0.0644 ± 0.0033	0.0401 ± 0.0065
d047	202.1286	-63.1310	19 281	0.0592 ± 0.0016	-0.0113 ± 0.0011	0.0198 ± 0.0030	0.0683 ± 0.0030	-0.0340 ± 0.0029	0.0581 ± 0.0020	-0.0535 ± 0.0024	0.0315 ± 0.0053
d048	205.2976	-62.8863	15 980	0.0510 ± 0.0021	-0.0185 ± 0.0011	0.0726 ± 0.0042	0.0526 ± 0.0032	-0.0170 ± 0.0042	0.0519 ± 0.0022	-0.0818 ± 0.0036	0.0373 ± 0.0056
d049	208.4062	-62.5724	8104	0.0770 ± 0.0037	-0.0217 ± 0.0017	0.0892 ± 0.0077	0.0592 ± 0.0056	-0.0487 ± 0.0078	0.0529 ± 0.0036	-0.1343 ± 0.0066	0.0391 ± 0.0086
d050	211.4437	-62.1913	7035	0.0664 ± 0.0040	-0.0299 ± 0.0019	0.0770 ± 0.0089	0.0566 ± 0.0062	0.0078 ± 0.0089	0.0483 ± 0.0041	-0.0777 ± 0.0070	0.0390 ± 0.0097
d051	214.3995	-61.7459	10 048	0.0546 ± 0.0029	-0.0154 ± 0.0014	0.0862 ± 0.0063	0.0364 ± 0.0046	0.0035 ± 0.0062	0.0357 ± 0.0030	-0.0660 ± 0.0048	0.0113 ± 0.0070
d052	217.2655	-61.2391	6859	0.0547 ± 0.0035	-0.0259 ± 0.0018	0.0950 ± 0.0070	0.0468 ± 0.0054	0.0140 ± 0.0071	0.0439 ± 0.0037	-0.0725 ± 0.0054	0.0252 ± 0.0083

Table B.2. continued.

Tile	RA (deg)	Dec (deg)	N_{fit}	α_K (mag)	β_K	α_{JH} (mag)	β_{JH}	α_{JK} (mag)	β_{JK}	α_{HK} (mag)	β_{HK}
d053	220.0361	-60.6742	8747	0.0506 ± 0.0028	-0.0260 ± 0.0015	0.0623 ± 0.0057	0.0643 ± 0.0045	0.0001 ± 0.0057	0.0483 ± 0.0030	-0.0629 ± 0.0044	0.0135 ± 0.0069
d054	222.7065	-60.0543	12 863	0.0627 ± 0.0028	-0.0277 ± 0.0013	0.0670 ± 0.0058	0.0485 ± 0.0041	0.0055 ± 0.0057	0.0407 ± 0.0028	-0.0694 ± 0.0045	0.0338 ± 0.0066
d055	225.2751	-59.3830	8754	0.0694 ± 0.0035	-0.0327 ± 0.0016	0.1346 ± 0.0079	0.0270 ± 0.0056	0.0480 ± 0.0078	0.0338 ± 0.0037	-0.0883 ± 0.0058	0.0485 ± 0.0082
d056	227.7405	-58.6635	11 901	0.0288 ± 0.0029	-0.0109 ± 0.0014	0.0977 ± 0.0059	0.0407 ± 0.0043	0.0396 ± 0.0060	0.0351 ± 0.0030	-0.0588 ± 0.0047	0.0213 ± 0.0071
d057	230.1038	-57.8993	9906	0.0268 ± 0.0038	-0.0098 ± 0.0020	0.0721 ± 0.0071	0.0659 ± 0.0056	-0.0059 ± 0.0071	0.0537 ± 0.0038	-0.0465 ± 0.0058	-0.0207 ± 0.0093
d058	232.3647	-57.0907	14 580	0.0436 ± 0.0034	-0.0254 ± 0.0016	0.0884 ± 0.0069	0.0438 ± 0.0049	0.0185 ± 0.0069	0.0440 ± 0.0033	-0.0390 ± 0.0053	-0.0006 ± 0.0077
d059	234.5306	-56.2485	11 191	0.0199 ± 0.0034	-0.0057 ± 0.0017	0.0754 ± 0.0072	0.0495 ± 0.0052	0.0110 ± 0.0069	0.0503 ± 0.0034	-0.0436 ± 0.0053	0.0149 ± 0.0080
d060	236.5999	-55.3681	9867	0.0737 ± 0.0033	-0.0256 ± 0.0016	0.0793 ± 0.0068	0.0313 ± 0.0050	0.0110 ± 0.0067	0.0328 ± 0.0033	-0.0705 ± 0.0055	0.0384 ± 0.0082
d061	238.5781	-54.4544	8220	0.0699 ± 0.0029	-0.0202 ± 0.0014	0.0568 ± 0.0056	0.0415 ± 0.0042	0.0006 ± 0.0057	0.0379 ± 0.0029	-0.0509 ± 0.0047	0.0179 ± 0.0073
d062	240.4685	-53.5101	4128	0.0688 ± 0.0051	-0.0200 ± 0.0025	0.0626 ± 0.0106	0.0664 ± 0.0081	-0.0405 ± 0.0106	0.0674 ± 0.0054	-0.0761 ± 0.0081	0.0286 ± 0.0123
d063	242.2762	-52.5375	4902	0.0577 ± 0.0041	-0.0192 ± 0.0023	0.1086 ± 0.0081	0.0258 ± 0.0068	0.0228 ± 0.0079	0.0333 ± 0.0045	-0.0802 ± 0.0065	0.0408 ± 0.0111
d064	244.0048	-51.5388	5123	0.1040 ± 0.0040	-0.0049 ± 0.0024	-0.0016 ± 0.0082	0.0568 ± 0.0072	-0.0523 ± 0.0079	0.0351 ± 0.0047	-0.0644 ± 0.0062	0.0169 ± 0.0116
d065	245.6584	-50.5163	5173	0.1124 ± 0.0051	-0.0112 ± 0.0024	0.0743 ± 0.0106	0.0225 ± 0.0075	-0.0301 ± 0.0104	0.0354 ± 0.0049	-0.0828 ± 0.0087	0.0309 ± 0.0124
d066	247.2417	-49.4715	5176	0.0994 ± 0.0054	-0.0274 ± 0.0026	0.0920 ± 0.0106	0.0594 ± 0.0080	-0.0427 ± 0.0107	0.0621 ± 0.0053	-0.1191 ± 0.0096	0.0447 ± 0.0136
d067	248.7586	-48.4061	2554	0.0547 ± 0.0061	-0.0151 ± 0.0031	0.0737 ± 0.0114	0.0605 ± 0.0089	-0.0153 ± 0.0114	0.0511 ± 0.0058	-0.0647 ± 0.0106	-0.0069 ± 0.0160
d068	250.2109	-47.3193	5466	0.0519 ± 0.0041	-0.0104 ± 0.0020	0.0588 ± 0.0077	0.0234 ± 0.0057	0.0105 ± 0.0075	0.0247 ± 0.0038	-0.0474 ± 0.0065	0.0273 ± 0.0103
d069	251.6072	-46.2182	4326	0.0229 ± 0.0047	-0.0132 ± 0.0022	0.1518 ± 0.0087	0.0022 ± 0.0060	0.0787 ± 0.0091	0.0146 ± 0.0042	-0.0682 ± 0.0083	0.0357 ± 0.0114
d070	252.9503	-45.1027	668	0.5558 ± 0.0263	-0.0284 ± 0.0095	-0.3473 ± 0.0651	-0.0200 ± 0.0322	-0.3103 ± 0.0647	-0.0104 ± 0.0238	0.0474 ± 0.0396	0.0008 ± 0.0573
d071	254.2399	-43.9703	7857	0.0576 ± 0.0034	-0.0170 ± 0.0016	0.0973 ± 0.0067	0.0372 ± 0.0048	0.0167 ± 0.0067	0.0340 ± 0.0032	-0.0717 ± 0.0059	0.0136 ± 0.0083
d072	255.4811	-42.8240	4962	0.0596 ± 0.0051	-0.0201 ± 0.0022	0.1490 ± 0.0116	0.0041 ± 0.0075	0.0612 ± 0.0121	0.0164 ± 0.0052	-0.0772 ± 0.0096	0.0263 ± 0.0121
d073	256.6775	-41.6650	5616	0.1245 ± 0.0047	-0.0320 ± 0.0022	0.1070 ± 0.0096	0.0118 ± 0.0067	-0.0142 ± 0.0100	0.0292 ± 0.0046	-0.1121 ± 0.0085	0.0492 ± 0.0116
d074	257.8319	-40.4943	8101	0.0953 ± 0.0051	-0.0256 ± 0.0026	0.1186 ± 0.0091	0.0027 ± 0.0069	-0.0244 ± 0.0096	0.0461 ± 0.0050	-0.0621 ± 0.0085	0.0122 ± 0.0136
d075	258.9468	-39.3125	4276	0.0839 ± 0.0071	-0.0079 ± 0.0041	0.0373 ± 0.0127	0.0832 ± 0.0108	-0.0612 ± 0.0126	0.0681 ± 0.0072	-0.0011 ± 0.0105	-0.1314 ± 0.0183
d076	260.0247	-38.1209	2970	0.1531 ± 0.0074	-0.0153 ± 0.0036	-0.0211 ± 0.0135	0.0405 ± 0.0095	-0.0990 ± 0.0140	0.0481 ± 0.0068	-0.0622 ± 0.0120	0.0404 ± 0.0188
d077	177.0402	-61.4155	7584	0.0491 ± 0.0047	-0.0277 ± 0.0034	0.1192 ± 0.0078	-0.0264 ± 0.0082	-0.0057 ± 0.0081	0.0486 ± 0.0059	-0.0168 ± 0.0064	-0.0438 ± 0.0153
d078	180.0302	-61.7369	11 200	-0.0079 ± 0.0037	0.0135 ± 0.0025	0.1472 ± 0.0060	-0.0563 ± 0.0060	0.0104 ± 0.0062	0.0397 ± 0.0043	-0.0031 ± 0.0045	-0.0500 ± 0.0105
d079	183.0765	-61.9914	16 535	0.0158 ± 0.0029	0.0040 ± 0.0019	0.0480 ± 0.0050	0.0614 ± 0.0048	-0.0018 ± 0.0051	0.0459 ± 0.0033	-0.0447 ± 0.0040	0.0003 ± 0.0083
d080	186.1673	-62.1775	10 912	0.0128 ± 0.0031	-0.0038 ± 0.0018	0.0609 ± 0.0062	0.0526 ± 0.0053	0.0142 ± 0.0058	0.0405 ± 0.0034	-0.0524 ± 0.0045	0.0244 ± 0.0082
d081	189.2895	-62.2934	10 466	0.0223 ± 0.0037	-0.0021 ± 0.0018	0.0767 ± 0.0079	0.0386 ± 0.0057	0.0298 ± 0.0075	0.0259 ± 0.0037	-0.0500 ± 0.0057	0.0010 ± 0.0085
d082	192.4280	-62.3390	9271	0.0310 ± 0.0034	-0.0034 ± 0.0016	0.1012 ± 0.0070	0.0344 ± 0.0050	0.0174 ± 0.0069	0.0273 ± 0.0033	-0.0627 ± 0.0056	-0.0163 ± 0.0078
d083	195.5693	-62.3131	6526	-0.0058 ± 0.0038	-0.0091 ± 0.0018	0.1004 ± 0.0083	0.0353 ± 0.0059	0.0410 ± 0.0080	0.0320 ± 0.0038	-0.0409 ± 0.0060	-0.0014 ± 0.0087
d084	198.6969	-62.2164	6914	0.0387 ± 0.0040	0.0025 ± 0.0019	0.0283 ± 0.0084	0.0508 ± 0.0058	-0.0066 ± 0.0080	0.0327 ± 0.0038	-0.0284 ± 0.0062	-0.0180 ± 0.0093
d085	201.7978	-62.0493	11 319	0.0380 ± 0.0025	-0.0208 ± 0.0013	0.0791 ± 0.0055	0.0492 ± 0.0043	0.0160 ± 0.0052	0.0386 ± 0.0027	-0.0604 ± 0.0040	0.0143 ± 0.0066
d086	204.8578	-61.8133	13 784	0.0367 ± 0.0025	-0.0099 ± 0.0013	0.0628 ± 0.0055	0.0616 ± 0.0042	0.0186 ± 0.0053	0.0366 ± 0.0027	-0.0430 ± 0.0040	-0.0153 ± 0.0063
d087	207.8637	-61.5103	7113	0.0763 ± 0.0043	-0.0180 ± 0.0019	0.1015 ± 0.0095	0.0312 ± 0.0064	-0.0052 ± 0.0095	0.0379 ± 0.0043	-0.0706 ± 0.0071	0.0032 ± 0.0093
d088	210.8059	-61.1419	2397	-0.0152 ± 0.0078	-0.0080 ± 0.0034	0.0974 ± 0.0188	0.0332 ± 0.0125	0.0698 ± 0.0177	0.0186 ± 0.0079	-0.0271 ± 0.0131	-0.0122 ± 0.0178
d089	213.6747	-60.7109	7249	0.0380 ± 0.0038	-0.0064 ± 0.0017	0.0881 ± 0.0085	0.0147 ± 0.0056	0.0383 ± 0.0083	0.0192 ± 0.0037	-0.0350 ± 0.0062	0.0076 ± 0.0086
d090	216.4618	-60.2201	8799	0.0205 ± 0.0031	-0.0158 ± 0.0015	0.0873 ± 0.0064	0.0561 ± 0.0047	0.0212 ± 0.0065	0.0478 ± 0.0032	-0.0506 ± 0.0049	0.0060 ± 0.0073
d091	219.1617	-59.6721	11 571	0.0365 ± 0.0027	-0.0211 ± 0.0013	0.0890 ± 0.0056	0.0470 ± 0.0041	0.0322 ± 0.0056	0.0361 ± 0.0028	-0.0510 ± 0.0042	0.0069 ± 0.0062
d092	221.7703	-59.0704	11 036	0.0485 ± 0.0028	-0.0220 ± 0.0014	0.0921 ± 0.0061	0.0279 ± 0.0044	0.0307 ± 0.0059	0.0335 ± 0.0029	-0.0567 ± 0.0043	0.0404 ± 0.0066
d093	224.2852	-58.4179	15 860	0.0564 ± 0.0023	-0.0086 ± 0.0011	0.0614 ± 0.0046	0.0358 ± 0.0035	0.0099 ± 0.0046	0.0232 ± 0.0023	-0.0571 ± 0.0035	0.0068 ± 0.0055
d094	226.7048	-57.7177	14 203	0.0417 ± 0.0032	-0.0096 ± 0.0015	0.0778 ± 0.0064	0.0383 ± 0.0046	0.0227 ± 0.0065	0.0339 ± 0.0032	-0.0539 ± 0.0049	0.0202 ± 0.0074
d095	229.0299	-56.9725	10 046	0.0871 ± 0.0040	-0.0335 ± 0.0019	0.0850 ± 0.0084	0.0436 ± 0.0060	-0.0066 ± 0.0085	0.0503 ± 0.0041	-0.0671 ± 0.0065	0.0272 ± 0.0096
d096	231.2605	-56.1861	11 300	0.0479 ± 0.0036	-0.0107 ± 0.0017	0.0748 ± 0.0068	0.0448 ± 0.0049	0.0015 ± 0.0070	0.0430 ± 0.0034	-0.0492 ± 0.0061	0.0044 ± 0.0090
d097	233.3992	-55.3605	13 335	0.0566 ± 0.0035	-0.0035 ± 0.0016	0.0502 ± 0.0070	0.0442 ± 0.0047	-0.0116 ± 0.0071	0.0309 ± 0.0033	-0.0307 ± 0.0055	-0.0410 ± 0.0076
d098	235.4482	-54.4991	3102	0.1133 ± 0.0067	-0.0317 ± 0.0028	0.0449 ± 0.0152	0.0311 ± 0.0093	-0.0257 ± 0.0154	0.0355 ± 0.0064	-0.0373 ± 0.0119	0.0057 ± 0.0150
d099	237.4110	-53.6041	4042	0.0715 ± 0.0058	-0.0124 ± 0.0023	0.1035 ± 0.0142	0.0041 ± 0.0083	0.0245 ± 0.0142	0.0172 ± 0.0055	-0.0686 ± 0.0102	0.0324 ± 0.0122
d100	239.2881	-52.6754	2651	0.8067 ± 0.0157	-0.0309 ± 0.0058	-0.0957 ± 0.0271	0.0091 ± 0.0176	-0.6261 ± 0.0338	0.0296 ± 0.0126	-0.5093 ± 0.0319	0.0350 ± 0.0279
d101	241.0900	-51.7235	5033	0.0075 ± 0.0052	-0.0150 ± 0.0023	0.1076 ± 0.0106	0.0383 ± 0.0071	0.0713 ± 0.0109	0.0328 ± 0.0049	-0.0269 ± 0.0083	0.0056 ± 0.0112
d102	242.8142	-50.7420	1913	0.0541 ± 0.0080	-0.0213 ± 0.0032	0.1847 ± 0.0184	-0.0169 ± 0.0113	0.1022 ± 0.0185	0.0044 ± 0.0075	-0.0778 ± 0.0140	0.0415 ± 0.0167
d103	244.4659	-49.7361	1392	0.2445 ± 0.0147	-0.0414 ± 0.0057	0.1196 ± 0.0307	-0.0125 ± 0.0188	-0.0511 ± 0.0330	-0.0020 ± 0.0131	-0.1164 ± 0.0247	-0.0367 ± 0.0272
d104	246.0499	-48.7074	2450	0.0785 ± 0.0094	-0.0250 ± 0.0042	0.0689 ± 0.0200	0.0552 ± 0.0133	-0.0043 ± 0.0201	0.0437 ± 0.0090	-0.0638 ± 0.0152	0.0070 ± 0.0205
d105	247.5690	-47.6577	5528	0.0804 ± 0.0054	-0.0167 ± 0.0025	0.0475 ± 0.0096	0.0532 ± 0.0067	-0.0121 ± 0.0098	0.0419 ± 0.0047	-0.0557 ± 0.0085	

Table B.2. continued.

Tile	RA (deg)	Dec (deg)	N_{fit}	α_K (mag)	β_K	α_{JH} (mag)	β_{JH}	α_{JK} (mag)	β_{JK}	α_{HK} (mag)	β_{HK}
d107	250.4290	-45.5011	4360	0.1155 ± 0.0070	-0.0040 ± 0.0034	0.0125 ± 0.0141	0.0433 ± 0.0102	-0.0492 ± 0.0136	0.0409 ± 0.0068	-0.0487 ± 0.0105	0.0149 ± 0.0167
d108	251.7765	-44.3972	4094	0.0402 ± 0.0066	0.0036 ± 0.0031	0.1045 ± 0.0137	0.0310 ± 0.0096	0.0345 ± 0.0136	0.0219 ± 0.0064	-0.0986 ± 0.0113	0.0445 ± 0.0159
d109	253.0732	-43.2775	5820	0.0283 ± 0.0044	-0.0009 ± 0.0020	0.1089 ± 0.0091	0.0064 ± 0.0060	0.0665 ± 0.0092	0.0049 ± 0.0041	-0.0398 ± 0.0076	-0.0012 ± 0.0104
d110	254.3225	-42.1437	3650	0.2672 ± 0.0078	-0.0106 ± 0.0031	-0.0834 ± 0.0161	0.0181 ± 0.0093	-0.1622 ± 0.0160	0.0212 ± 0.0064	-0.0537 ± 0.0126	-0.0032 ± 0.0160
d111	255.5272	-40.9968	3908	0.1787 ± 0.0072	-0.0251 ± 0.0028	0.0691 ± 0.0158	0.0018 ± 0.0093	-0.0423 ± 0.0163	0.0182 ± 0.0064	-0.0974 ± 0.0123	0.0345 ± 0.0146
d112	256.6880	-39.8348	3404	0.0073 ± 0.0073	-0.0136 ± 0.0031	0.1377 ± 0.0155	0.0063 ± 0.0098	0.0974 ± 0.0157	0.0030 ± 0.0067	-0.0570 ± 0.0133	0.0206 ± 0.0171
d113	257.8140	-38.6664	6985	0.0961 ± 0.0047	-0.0305 ± 0.0023	0.0640 ± 0.0090	0.0426 ± 0.0064	-0.0190 ± 0.0089	0.0498 ± 0.0043	-0.0695 ± 0.0080	0.0420 ± 0.0120
d114	258.9010	-37.4849	6355	0.1113 ± 0.0040	-0.0262 ± 0.0021	0.0006 ± 0.0068	0.0573 ± 0.0051	-0.0445 ± 0.0070	0.0518 ± 0.0036	-0.0608 ± 0.0063	0.0645 ± 0.0105
d115	177.5766	-60.3547	9115	0.0283 ± 0.0053	-0.0149 ± 0.0050	0.0789 ± 0.0071	-0.0189 ± 0.0092	0.0042 ± 0.0075	0.0363 ± 0.0071	0.0488 ± 0.0053	-0.2629 ± 0.0180
d116	180.4729	-60.6657	13 612	0.0101 ± 0.0035	0.0133 ± 0.0030	0.0523 ± 0.0049	0.0610 ± 0.0061	-0.0113 ± 0.0052	0.0471 ± 0.0044	-0.0478 ± 0.0045	-0.0327 ± 0.0121
d117	183.4198	-60.9115	15 327	0.0190 ± 0.0032	-0.0032 ± 0.0026	0.0603 ± 0.0048	0.0371 ± 0.0055	0.0347 ± 0.0049	0.0158 ± 0.0039	-0.0235 ± 0.0040	-0.0416 ± 0.0108
d118	186.4069	-61.0913	14 084	0.0118 ± 0.0031	0.0067 ± 0.0027	0.0437 ± 0.0046	0.0483 ± 0.0056	0.0189 ± 0.0047	0.0247 ± 0.0041	-0.0265 ± 0.0038	-0.0334 ± 0.0115
d119	189.4216	-61.2032	12 454	0.0073 ± 0.0025	0.0048 ± 0.0017	0.0666 ± 0.0046	0.0283 ± 0.0047	0.0377 ± 0.0044	0.0158 ± 0.0031	-0.0299 ± 0.0034	-0.0086 ± 0.0078
d120	192.4518	-61.2469	13 745	0.0334 ± 0.0022	-0.0084 ± 0.0013	0.0513 ± 0.0043	0.0523 ± 0.0038	0.0103 ± 0.0041	0.0309 ± 0.0025	-0.0437 ± 0.0032	-0.0102 ± 0.0059
d121	195.4831	-61.2217	15 494	0.0435 ± 0.0020	-0.0106 ± 0.0011	0.0694 ± 0.0041	0.0326 ± 0.0033	0.0128 ± 0.0040	0.0266 ± 0.0022	-0.0501 ± 0.0030	0.0017 ± 0.0051
d122	198.5034	-61.1281	10 338	0.0223 ± 0.0027	-0.0105 ± 0.0015	0.0730 ± 0.0056	0.0437 ± 0.0045	0.0372 ± 0.0053	0.0251 ± 0.0029	-0.0424 ± 0.0039	-0.0055 ± 0.0067
d123	201.4990	-60.9663	18 271	0.0293 ± 0.0020	-0.0115 ± 0.0014	0.0667 ± 0.0038	0.0359 ± 0.0040	0.0240 ± 0.0036	0.0308 ± 0.0026	-0.0409 ± 0.0029	0.0118 ± 0.0069
d124	204.4580	-60.7383	18 463	0.0053 ± 0.0026	0.0063 ± 0.0017	0.0839 ± 0.0047	0.0347 ± 0.0045	0.0533 ± 0.0044	0.0127 ± 0.0029	-0.0224 ± 0.0036	-0.0547 ± 0.0078
d125	207.3688	-60.4448	20 055	0.0343 ± 0.0026	-0.0051 ± 0.0017	0.0717 ± 0.0046	0.0362 ± 0.0043	0.0055 ± 0.0045	0.0394 ± 0.0029	-0.0642 ± 0.0038	0.0387 ± 0.0078
d126	210.2215	-60.0880	5087	0.0052 ± 0.0053	-0.0159 ± 0.0034	0.0664 ± 0.0105	0.0446 ± 0.0098	0.0278 ± 0.0097	0.0373 ± 0.0062	-0.0135 ± 0.0078	-0.0269 ± 0.0160
d127	213.0073	-59.6704	18 339	0.0193 ± 0.0028	-0.0063 ± 0.0017	0.0609 ± 0.0051	0.0600 ± 0.0046	0.0129 ± 0.0050	0.0401 ± 0.0031	-0.0431 ± 0.0040	-0.0114 ± 0.0077
d128	215.7194	-59.1940	19 165	0.0334 ± 0.0032	-0.0149 ± 0.0020	0.0678 ± 0.0057	0.0479 ± 0.0052	0.0099 ± 0.0056	0.0409 ± 0.0035	-0.0455 ± 0.0046	0.0032 ± 0.0092
d129	218.3517	-58.6620	20 550	0.0336 ± 0.0033	-0.0083 ± 0.0021	0.0624 ± 0.0055	0.0462 ± 0.0052	0.0029 ± 0.0056	0.0422 ± 0.0036	-0.0334 ± 0.0047	-0.0245 ± 0.0100
d130	220.9005	-58.0769	23 516	0.0097 ± 0.0027	0.0179 ± 0.0020	0.0808 ± 0.0045	0.0135 ± 0.0046	0.0352 ± 0.0045	0.0143 ± 0.0033	-0.0340 ± 0.0037	-0.0194 ± 0.0092
d131	223.3630	-57.4416	20 151	0.0038 ± 0.0033	0.0095 ± 0.0022	0.0767 ± 0.0058	0.0307 ± 0.0055	0.0226 ± 0.0057	0.0295 ± 0.0038	-0.0396 ± 0.0044	-0.0055 ± 0.0095
d132	225.7375	-56.7590	20 501	-0.0129 ± 0.0029	0.0202 ± 0.0018	0.1254 ± 0.0052	-0.0115 ± 0.0046	0.0688 ± 0.0051	0.0022 ± 0.0032	-0.0182 ± 0.0041	-0.0426 ± 0.0083
d133	228.0234	-56.0321	21 311	0.0084 ± 0.0023	0.0054 ± 0.0013	0.0969 ± 0.0044	0.0192 ± 0.0037	0.0428 ± 0.0044	0.0190 ± 0.0026	-0.0536 ± 0.0034	0.0187 ± 0.0062
d134	230.2212	-55.2638	22 417	0.0129 ± 0.0023	0.0133 ± 0.0015	0.0871 ± 0.0039	0.0180 ± 0.0037	0.0247 ± 0.0040	0.0264 ± 0.0026	-0.0527 ± 0.0035	0.0199 ± 0.0073
d135	232.3327	-54.4564	22 477	0.0160 ± 0.0021	0.0054 ± 0.0013	0.0814 ± 0.0038	0.0218 ± 0.0034	0.0189 ± 0.0038	0.0286 ± 0.0023	-0.0596 ± 0.0031	0.0323 ± 0.0061
d136	234.3604	-53.6129	16 827	0.0231 ± 0.0026	0.0050 ± 0.0015	0.0788 ± 0.0047	0.0223 ± 0.0042	0.0288 ± 0.0047	0.0235 ± 0.0029	-0.0428 ± 0.0039	0.0080 ± 0.0076
d137	236.3054	-52.7358	11 796	0.0293 ± 0.0025	-0.0051 ± 0.0014	0.0586 ± 0.0053	0.0527 ± 0.0044	0.0097 ± 0.0050	0.0401 ± 0.0028	-0.0430 ± 0.0040	-0.0002 ± 0.0070
d138	238.1700	-51.8245	10 574	0.0188 ± 0.0027	-0.0053 ± 0.0014	0.0712 ± 0.0062	0.0449 ± 0.0046	0.0139 ± 0.0060	0.0358 ± 0.0030	-0.0566 ± 0.0045	0.0148 ± 0.0070
d139	239.9601	-50.8868	12 289	0.0288 ± 0.0028	-0.0087 ± 0.0015	0.0517 ± 0.0054	0.0498 ± 0.0042	-0.0095 ± 0.0053	0.0507 ± 0.0029	-0.0453 ± 0.0041	0.0205 ± 0.0070
d140	241.6791	-49.9245	6530	-0.0367 ± 0.0046	0.0173 ± 0.0024	0.1171 ± 0.0093	0.0194 ± 0.0074	0.1122 ± 0.0089	-0.0088 ± 0.0048	-0.0099 ± 0.0071	-0.0585 ± 0.0118
d141	243.3271	-48.9346	15 508	0.0633 ± 0.0027	-0.0253 ± 0.0014	0.0826 ± 0.0056	0.0270 ± 0.0043	0.0190 ± 0.0053	0.0356 ± 0.0028	-0.0458 ± 0.0042	0.0218 ± 0.0071
d142	244.9090	-47.9215	17 346	0.0359 ± 0.0026	-0.0003 ± 0.0016	0.0413 ± 0.0050	0.0380 ± 0.0045	0.0060 ± 0.0046	0.0334 ± 0.0029	-0.0074 ± 0.0038	-0.0436 ± 0.0080
d143	246.4288	-46.8865	8065	-0.0056 ± 0.0048	0.0272 ± 0.0034	0.0667 ± 0.0086	0.0226 ± 0.0086	0.0499 ± 0.0080	0.0054 ± 0.0057	0.0121 ± 0.0063	-0.1105 ± 0.0156
d144	247.8894	-45.8315	22 865	0.0497 ± 0.0031	-0.0142 ± 0.0022	0.0589 ± 0.0052	0.0480 ± 0.0052	0.0071 ± 0.0051	0.0404 ± 0.0036	-0.0234 ± 0.0044	-0.0497 ± 0.0102
d145	249.2940	-44.7579	20 997	-0.0018 ± 0.0031	0.0189 ± 0.0022	0.1079 ± 0.0054	-0.0052 ± 0.0055	0.0494 ± 0.0052	0.0107 ± 0.0037	-0.0305 ± 0.0045	-0.0218 ± 0.0105
d146	250.6457	-43.6672	18 368	-0.0106 ± 0.0028	0.0068 ± 0.0018	0.0847 ± 0.0052	0.0310 ± 0.0047	0.0647 ± 0.0049	0.0200 ± 0.0031	0.0008 ± 0.0042	-0.0492 ± 0.0086
d147	251.9480	-42.5603	13 012	0.0180 ± 0.0031	-0.0007 ± 0.0019	0.0829 ± 0.0063	0.0446 ± 0.0056	0.0533 ± 0.0058	0.0120 ± 0.0035	-0.0110 ± 0.0048	-0.0916 ± 0.0091
d148	253.2033	-41.4384	5479	0.0547 ± 0.0038	-0.0238 ± 0.0026	0.0656 ± 0.0075	0.0467 ± 0.0075	0.0087 ± 0.0070	0.0391 ± 0.0048	-0.0525 ± 0.0056	0.0099 ± 0.0122
d149	254.4150	-40.3029	19 320	0.0312 ± 0.0018	-0.0095 ± 0.0010	0.0870 ± 0.0036	0.0307 ± 0.0029	0.0495 ± 0.0035	0.0169 ± 0.0019	-0.0404 ± 0.0028	-0.0066 ± 0.0046
d150	255.5831	-39.1525	15 334	0.0027 ± 0.0024	-0.0043 ± 0.0014	0.0893 ± 0.0047	0.0345 ± 0.0040	0.0422 ± 0.0045	0.0310 ± 0.0026	-0.0414 ± 0.0036	0.0105 ± 0.0067
d151	256.7141	-37.9917	18 430	0.0540 ± 0.0026	-0.0328 ± 0.0017	0.0518 ± 0.0051	0.0636 ± 0.0047	-0.0110 ± 0.0047	0.0619 ± 0.0030	-0.0450 ± 0.0041	0.0218 ± 0.0084
d152	257.8110	-36.8225	16 630	0.0107 ± 0.0029	0.0002 ± 0.0017	0.1146 ± 0.0055	0.0144 ± 0.0049	0.0344 ± 0.0054	0.0324 ± 0.0032	-0.0666 ± 0.0044	0.0444 ± 0.0084

Appendix C: Variation of the photometric coefficients per tile

Thus far we presented photometric transformations calculated for each tile. Here we explore the variation of the transformation coefficients across single tiles. We divided a complete tile in 64 (8×8) parts. Each of these 64 sub-fields (1597×1957 pixels) was used to calculate the transformation coefficients with the same procedure applied to complete tiles. We chose two tiles with different reddening, namely tiles d003 and d050 (with modified SFD reddening $E(B-V) \approx 1.18$ and $E(B-V) \approx 3.29$, respectively). The average and dispersion, which for both fields are shown in Table C.1, were weighted by the number of stars per sub-tile. Figure C.1 shows the map of the coefficients for tile d003. In general, there is general agreement between the average of the coefficients and those calculated for the complete field (Table A.1). In some cases the variations are beyond the error bars, which may be attributed to population and extinction variations, or small statistics (~ 300 stars) per sub-field. Furthermore, the observed weighted dispersion displays similar values for most of the coefficients ~ 0.02 mag, with the exception of β_{HK} , which exhibits a dispersion three times larger (~ 0.06 mag). Again, the observed dispersion in β_{HK} (Fig. 8) appears sensitive to extinction.

Table C.1. Average and dispersion of transformation coefficients between 2MASS and VVV photometric systems for 104 subfields in tiles d003 and d050.

Coeff	d003		d050	
	avg	Sdev	avg	Sdev
α_K	0.0331 ± 0.0027	0.0221 ± 0.0017	0.0423 ± 0.0029	0.0237 ± 0.0020
β_K	-0.0103 ± 0.0018	0.0140 ± 0.0013	-0.0217 ± 0.0026	0.0227 ± 0.0037
α_{HK}	0.0135 ± 0.0024	0.0180 ± 0.0013	0.0511 ± 0.0028	0.0217 ± 0.0017
β_{HK}	0.0948 ± 0.0028	0.0238 ± 0.0027	0.0789 ± 0.0019	0.0153 ± 0.0014
α_{JK}	-0.0165 ± 0.0024	0.0200 ± 0.0016	-0.0241 ± 0.0027	0.0217 ± 0.0017
β_{JK}	0.0640 ± 0.0024	0.0195 ± 0.0018	0.0680 ± 0.0026	0.0206 ± 0.0025
α_{HK}	-0.0231 ± 0.0023	0.0184 ± 0.0016	-0.0708 ± 0.0033	0.0270 ± 0.0027
β_{HK}	-0.0340 ± 0.0061	0.0482 ± 0.0042	0.0352 ± 0.0067	0.0555 ± 0.0060

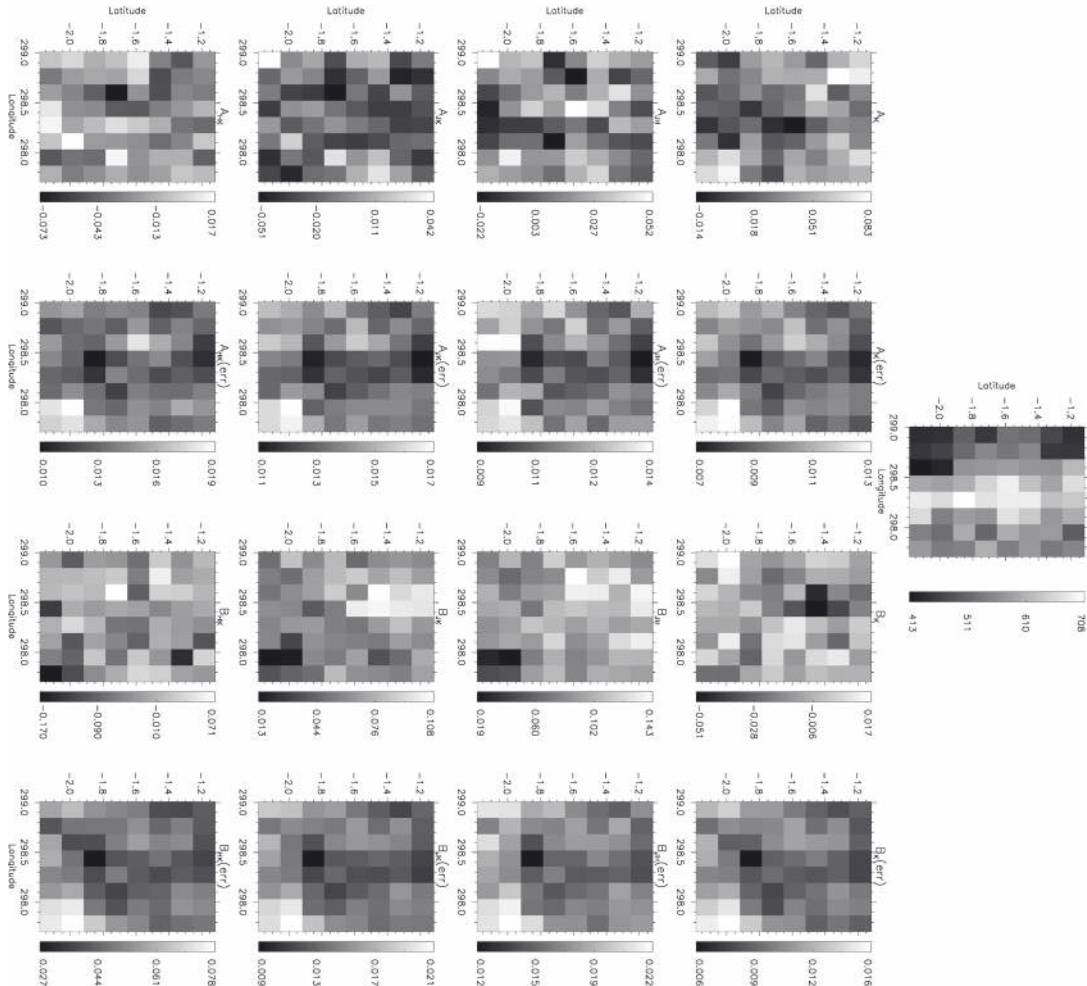


Fig. C.1. Variations of the coefficients for the photometric transformations across a single tile, tile d003. The complete tile has been divided in 64 parts (8×8). (*Top*), number of stars per sub-field. (*Second row to bottom*), map of coefficients of the photometric transformations and their respective errors.

Appendix D: Transformation coefficients divided by latitude and longitude

Table D.1. Fourth-order polynomial coefficients for the fitting of the photometric coefficients as a function of the Galactic longitude.

Coeff ^a	C_0	C_1	C_2	C_3	C_4
α_K ($ l < 1^\circ$)	-365.4430 ± 34.3853	4.4934 ± 0.4285	-2.0710e-02 ± 0.2000e-02	4.2407e-05 ± 0.4147e-05	-3.2551e-08 ± 0.3220e-08
β_K	18.8419 ± 2.72586	-0.1829 ± 0.3391	0.6150e-03 ± 1.5809e-03	-0.78657e-06 ± 3.2722e-06	2.3628e-10 ± 0.2538e-09
α_{JH}	-417.7458 ± 49.0418	5.2539 ± 0.6116	-2.4749e-02 ± 0.2858e-02	5.1752e-05 ± 0.5930e-05	-4.0528e-08 ± 0.4609e-08
β_{JH}	317.8541 ± 57.8718	-4.0524 ± 0.7205	1.9351e-02 ± 0.3360e-02	-4.1006e-05 ± 0.6960e-05	3.2553e-08 ± 0.5400e-08
α_{JK}	-41.0102 ± 52.1432	0.5933 ± 0.6501	-3.1379e-03 ± 3.0363e-03	7.2314e-06 ± 6.2971e-06	-6.1507e-09 ± 4.8930e-09
β_{JK}	424.2013 ± 42.5080	-5.3723 ± 0.5290	2.5478e-02 ± 0.2467e-02	-5.3618e-05 ± 0.5107e-05	4.2249e-08 ± 0.3962e-08
α_{HK}	843.9939 ± 50.2942	-10.4583 ± 0.6269	4.8559e-02 ± 0.2928e-02	-1.0013e-04 ± 0.0607e-04	7.7367e-08 ± 0.47178e-08
β_{HK}	-442.9768 ± 129.7205	5.3851 ± 1.6147	-2.4535e-02 ± 0.7530e-02	4.9048e-05 ± 1.5594e-05	-3.7649e-08 ± 1.2099e-08
α_K ($-2.1^\circ \geq b \geq 1^\circ$)	-1923.7242 ± 37.1316	24.1147 ± 0.4637	-1.1324e-01 ± 0.0217e-01	2.3610e-04 ± 0.0451e-04	-1.8439e-07 ± 0.0351e-07
β_K	15.0531 ± 25.7626	-0.1462 ± 0.3211	0.4969e-03 ± 1.4994e-03	-0.6634e-06 ± 3.1094e-06	0.2439e-09 ± 2.4160e-09
α_{JH}	-448.6523 ± 55.9766	5.5559 ± 0.6994	-2.5813e-02 ± 0.3274e-02	5.3338e-05 ± 0.6807e-05	-4.1360e-08 ± 0.5302e-08
β_{JH}	588.0175 ± 59.3255	-7.3890 ± 0.7397	3.4798e-02 ± 0.3456e-02	-7.2778e-05 ± 0.7170e-05	5.7031e-08 ± 0.5573e-08
α_{JK}	1402.2977 ± 59.4223	-17.4729 ± 0.7424	8.1554e-02 ± 0.3475e-02	-1.6899e-04 ± 0.0722e-04	1.3115e-07 ± 0.0563e-07
β_{JK}	250.0838 ± 42.4663	-3.1881 ± 0.5294	1.5220e-02 ± 0.2473e-02	-3.2238e-05 ± 0.51130e-05	2.5564e-08 ± 0.3987e-08
α_{HK}	1462.7836 ± 56.5467	-18.1479 ± 0.7064	8.4378e-02 ± 0.3306e-02	-1.7420e-04 ± 0.0687e-04	1.3487e-07 ± 0.0335e-07
β_{HK}	-1269.9341 ± 122.9108	15.6974 ± 1.5323	-7.2724e-02 ± 0.7158e-02	1.4966e-04 ± 0.1485e-04	-1.1543e-07 ± 0.1154e-07

Notes. ^(a) Coefficients applied to a fitting equation of the form: $y = C_0 + C_1x + C_2x^2 + C_3x^3 + C_4x^4$, where $x = l$, the Galactic longitude.

Table D.2. Third-order polynomial coefficients for the fitting of the photometric coefficients as a function of the Galactic latitude.

Coeff ^a	C_0	C_1	C_2	C_3
α_K ($l \geq 320^\circ$)	8.7137e-02 ± 0.0248e-02	3.2361e-02 ± 0.0453e-02	-1.8083e-02 ± 0.0114e-02	-1.4078e-02 ± 0.0173e-02
β_K	-1.5320e-02 ± 0.0156e-02	-2.3980e-03 ± 0.2848e-03	1.6433e-03 ± 0.0769e-03	1.4568e-03 ± 0.1106e-03
α_{JH}	2.4836e-02 ± 0.0396e-02	-1.8102e-02 ± 0.0723e-02	9.2059e-04 ± 1.7754e-04	7.8366e-03 ± 0.2762e-03
β_{JH}	6.5333e-02 ± 0.0386e-02	-3.1511e-03 ± 0.7048e-03	2.8729e-03 ± 0.1817e-03	5.4973e-04 ± 2.7140e-04
α_{JK}	-5.6450e-02 ± 0.0415e-02	-2.5840e-02 ± 0.0756e-02	1.6496e-02 ± 0.0185e-02	1.1324e-02 ± 0.0289e-02
β_{JK}	5.4228e-02 ± 0.0269e-02	-1.8258e-03 ± 0.4919e-03	-7.0817e-04 ± 1.2830e-04	-2.8354e-04 ± 1.8979e-04
α_{HK}	-6.9442e-02 ± 0.0393e-02	-1.5938e-02 ± 0.0717e-02	1.3718e-02 ± 0.0177e-02	5.8553e-03 ± 0.2739e-03
β_{HK}	2.2701e-02 ± 0.0754e-02	6.9031e-03 ± 1.3767e-03	-1.2861e-02 ± 0.0374e-02	-2.4821e-03 ± 0.5351e-03
α_K ($l < 320^\circ$)	3.8479e-02 ± 0.0196e-02	-9.3109e-03 ± 0.3560e-03	-1.9789e-03 ± 0.1088e-03	1.9851e-03 ± 0.1415e-03
β_K	-1.3918e-02 ± 0.0141e-02	4.5106e-03 ± 0.2552e-03	1.9777e-03 ± 0.0875e-03	-1.3459e-03 ± 0.1043e-03
α_{JH}	3.6107e-02 ± 0.0293e-02	-4.8033e-03 ± 0.5342e-03	-5.9765e-03 ± 0.1543e-03	3.2205e-03 ± 0.2098e-03
β_{JH}	7.4869e-02 ± 0.0335e-02	-4.9043e-03 ± 0.6098e-03	2.9709e-03 ± 0.1888e-03	3.3755e-04 ± 2.4307e-04
α_{JK}	-2.4255e-02 ± 0.0316e-02	6.5936e-03 ± 0.5748e-03	2.8184e-03 ± 0.1670e-03	-5.2040e-04 ± 2.2604e-04
β_{JK}	5.6893e-02 ± 0.0240e-02	-5.2755e-03 ± 0.4366e-03	-6.8883e-04 ± 1.3891e-04	5.3354e-04 ± 1.7513e-04
α_{HK}	-5.6496e-02 ± 0.0299e-02	1.1284e-02 ± 0.0546e-02	9.4227e-03 ± 0.1601e-03	-4.1742e-03 ± 0.2150e-03
β_{HK}	1.4171e-02 ± 0.0665e-02	-7.1747e-03 ± 1.2078e-03	-1.4146e-02 ± 0.0409e-02	3.2066e-03 ± 0.4921e-03

Notes. ^(a) Coefficients applied to a fitting equation of the form: $y = C_0 + C_1x + C_2x^2 + C_3x^3$, where $x = b$, the Galactic latitude.